Spring 2022

Characterization of Functionalized Carbon Nanotubes and Polystyrene/CNT Composites Prepared with Microwave-Induced Polymerization

Allen Hulette

Recommended Citation

Hulette, Allen, "Characterization of Functionalized Carbon Nanotubes and Polystyrene/CNT Composites Prepared with Microwave-Induced Polymerization" (2022). *Electronic Theses and Dissertations*. 2419.
https://digitalcommons.georgiasouthern.edu/etd/2419

CHARACTERIZATION OF FUNCTIONALIZED CARBON NANOTUBES AND POLYSTYRENE/CNT COMPOSITES PREPARED WITH MICROWAVE-INDUCED POLYMERIZATION

by

ALLEN HULETTE

(Under the Direction of Rafael Quirino)

ABSTRACT

The use of carbon nanotubes in polymer composites can increase the mechanical properties of the resulting product. Carbon nanotubes are known to have chemical interactions that make them attracted to one another and aggregate. To reduce this agglomeration and disperse the mechanical properties throughout the composite, functional groups are covalently added to the carbon nanotubes. Another known property of carbon nanotubes is their ability to absorb microwaves and convert it into other forms of energy. This research investigates the effects of carbon nanotube absorption of microwaves and initiation of styrene polymerization. Grignard reactions are used to attach aromatic functional groups with and without vinyl side groups to investigate crosslinking of carbon nanotubes and styrene polymer chains. It is hypothesized that the functionalization of CNTs will reduce aggregation of nanoparticles in polystyrene composites and that polymerization of these composites can be induces with microwaves. It is expected that that microwave irradiation energy would be powerful enough to initiate stepwise polymerization starting at the carbon nanotube through the vinyl group. The double bonded carbon group found in styrenyl functionalized CNTs would theoretically be able to induce crosslinking with styrene monomers. The functionalization of carbon nanotubes is characterized with settling tests, thermogravimetric analysis (TGA), and Raman spectroscopy. The composites synthesized with functionalized carbon nanotubes are analyzed with TGA, dynamic mechanical analysis (DMA), differential scanning calorimetry (DSC), and X-Ray diffraction (XRD).

INDEX WORDS: Carbon nanotube, Polymer-matrix composites, Functionalization, Grignard reagent, Microwave polymerization, Mechanical properties

CHARACTERIZATION OF FUNCTIONALIZED CARBON NANOTUBES AND POLYSTYRENE/CNT COMPOSITES PREPARED WITH MICROWAVE-INDUCED POLYMERIZATION

by

ALLEN HULETTE

B. S., Georgia Southern University, 2020

A Thesis Submitted to the Graduate Faculty of Georgia Southern University in Partial

Fulfillment of the Requirements for the Degree

MASTER OF SCIENCE

COLLEGE OF SCIENCE AND MATHEMATICS

CHARACTERIZATION OF FUNCTIONALIZED CARBON NANOTUBES AND POLYSTYRENE/CNT COMPOSITES PREPARED WITH MICROWAVE-INDUCED POLYMERIZATION

by

ALLEN HULETTE

Major Professor: Rafael Quirino

Committee: John DiCesare

Ji Wu

Electronic Version Approved:

May 2022

DEDICATION

I dedicate this paper to my parents and grandparents for always supporting me through my academic career.

ACKNOWLEDGMENTS

I would like to thank Dr. Quirino for his expertise in polymer chemistry and for all of the research opportunities that were made available to me. I'd also like to thank Dr. DiCesare for his help in the lab with functionalization and expertise in organometallic reactions. My research committee helped me every step of the way in this thesis preparation, and I appreciate everything that they have done for me.

TABLE OF CONTENTS

LIST OF TABLES

LIST OF FIGURES

CHAPTER 1

LITERATURE REVIEW

1.1 Styrene

Styrene is a flammable, reactive, carcinogenic, organic compound. Styrene monomers can also instantaneously polymerize via chain reactions. The airborne permissible exposure limit (PEL) for styrene is 100 ppm over an 8-hour workshift, the recommended airborne exposure limit (REL) is 50 ppm over a 10-hour workshift, and the threshold limit value (TLV) is 20 ppm over an 8-hour workshift. These regulative workplace exposure limits are put into place by OSHA, NIOSH, and ACGIH.[1] Repeated exposures can result in concentration and memory problems along with slowed reflexes and confusion that can last up to a few years. Styrene is synthesized via reacting ethylene and benzene followed by the dehydrogenation of ethylbenzene.[2] Both ethylene and benzene are obtained as a byproduct of crude oil distillation. Styrene is considered the poster child of monomers due to its carbon-carbon double bond, or vinyl group, that allows it to produce long polymer chains that are supported by aromatic rings. Many polymer matrixes revolve around the presence of a vinyl group and have aromatic rings in their monomer. The aromatic rings found in monomers make the polymer structure more stable and increases the mechanical strength of the resulting polymer.

Styrene is commonly used in polymerization reactions due to the vinyl group attached to the aromatic ring of the styrene monomer.[3] Free radical initiators like benzoyl peroxide can be used to initiate the polymerization of styrene. Figure 1 shows how styrene monomer polymerization can propagate once a free radical is introduced due to the creation of relatively stable free radicals from the vinyl group. Since styrene tends to readily polymerize, the monomer needs to be stored in a refrigerator and polymerization inhibitors are commonly added to stock styrene bottles. This reduces the potential for free radical production and therefore spontaneous initiation of the polymer matrix.

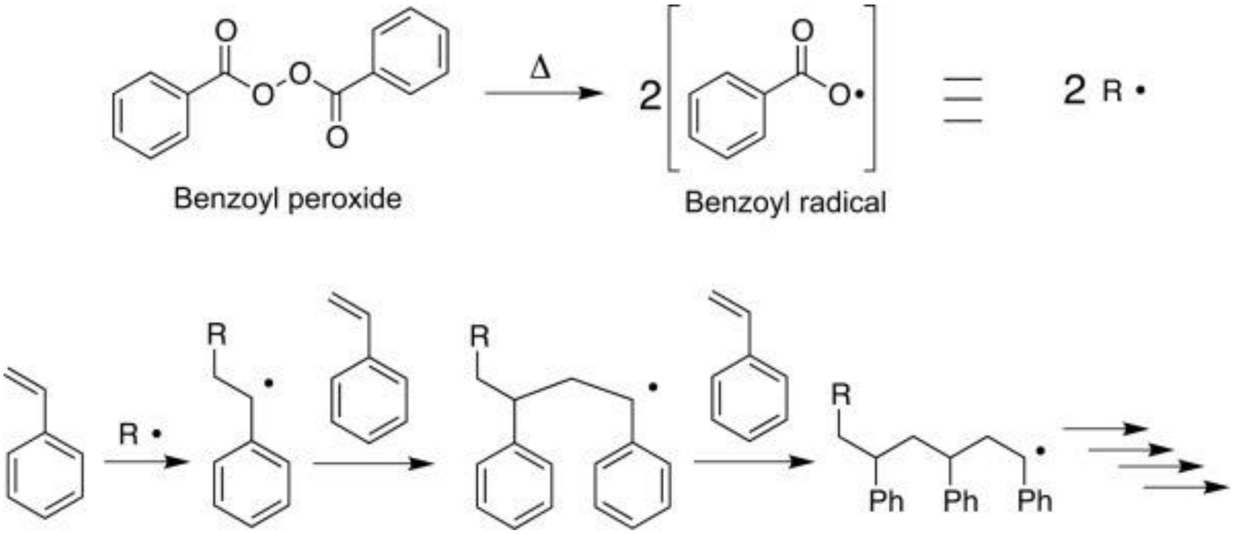

Figure 1. Polymerization mechanism of styrene. (Adapted from Isac-García et al. 2016)[4]

Styrene is currently readily available and easily produced because it is a direct byproduct of the petroleum industry. Polystyrene can be reinforced with many different types of materials, resulting in composites with different properties or even produce different types of physical forms out of polystyrene alone. One example of this is the synthesis of rigid polystyrene plastics versus the production of Styrofoam for packing peanuts. Both the rigid polystyrene and Styrofoam are made of polystyrene, but the Styrofoam is an expanded version that uses solvents and gases to decrease the density of the polymer structure.[5] A research team from Malaysia published a paper in 2019 investigating the use of expanded polystyrene as an application for the construction industry. The composites formed were found to be a good insulator that could easily be molded into precise shapes for decorative panels. These composites are similar to commonly used Styrofoam cups that also provide insulation.[5]

When it comes to producing strong polymers, the use of only styrene monomers results in relatively low mechanical properties due to the stiff polymer backbone of polystyrene. The covalently bonded vinyl groups of the styrene monomers create a structure that does not freely rotate and therefore breaks easily. This concept is readily accepted by the polymer science community; so, to study the effect of composite additives on mechanical properties, the study of polystyrene composites with pure styrene polymers as a baseline is useful.

Styrene monomer use is directly correlated to crude oil production. Many countries, including the United States, have pledged to reduce their carbon emissions in the coming years. Recently, oil prices have increased drastically due to a worldwide pandemic and international tensions with Russia. The long-term use of styrene monomers is not fully known but the use of them in the past has been prevalent as the most used monomer for polymer production for the past 20 years.[6] The continued use as a standard monomer will most likely continue for the foreseeable future but substitutes will eventually need to be found and/or an efficient recycling program of polystyrene will need to be developed. There is also a large mass of plastic currently in the ocean with no feasible way of recycling it efficiently. The recycling processes for styrene plastics has been a leading topic of funded research as of recent.[6] Efficient recycling processes for a mix of monomers has been a large obstacle for scientists trying to find a purpose for end-use plastics. Styrene monomers are used in this study because of the aromatic ring and vinyl group that the monomer possess. These attributes are commonly found in monomers so if the properties of functionalized carbon nanotubes can be applied to polystyrene composites, conceptually they can be applied to other polymer composites. There is a need for more efficient recycling processes of thermoplastics and the use of carbon nanotube absorption properties could be a route of pyrolysis of polymer chains.

1.2 Carbon Nanotubes (CNTs)

To fully understand carbon nanotubes and their relative history, it is useful to also understand the origins of nanotechnology. The concept of nanotechnology was first introduced in 1959 by Richard Feynman and it wasn't until 1986 that K. Eric Drexler published the first book on nanotechnology that described the approaches to nanoparticle creation. The two approaches used to synthesize these new types of nanostructures were top-down and bottom-up approaches where particles were produced by either breaking a large, repeating chemical structure into nanoparticles or the arrangement of atoms into nanostructures.[7] The first observed synthesis of carbon nanotubes was in 1991 by Sumio Iijima and was produced via arc discharge.[8]

While the theory of nanotechnology was not correctly put into a concept until the twentieth century, this does not mean that nanotechnology was not previously created and used. One of the most famous cases is that of the Lycurgus cup from the fourth century. The Roman originating cup is made of dichroic glass that changes color in different light settings due to the silver-gold alloy nanoparticles that either disperse or absorb different wavelength of light similar to medieval church windows.[7] The glass makers at the time did not fully understand the concept of nanoparticles and their light scattering mechanics, but their physical characteristics were still used. Damascus blades dating back to the first century BC in ancient India were found to contain carbon nanotubes. This production of Wootz steel was due to impurities present in the steel when it was being forged. This method of steel production creates a unique banding pattern of carbon-poor and carbon-rich zones.[9] It is one of the oldest methods of forging, yet it was not until recently that these carbon nanotube structures were discovered to be in to swords. Because of this, carbon nanotubes were most likely synthesized many times before 1991 but their concept and existence were not yet understood. The probability that CNTs were made in any large quantity before the 20th century are low due to the high amounts of energy required to form the structures. In the three decades since Sumio Iijima's discovery, carbon nanotubes have been greatly researched due to their thermal, mechanical, and electrical properties. There are many ways of creating carbon nanotubes, many of which being bottom-up approaches from a sample of graphite. The three most common ways are plasma arc discharge, chemical vapor deposition (CVD), and laser ablation.[10]

Plasma arc discharge

Plasma arc discharge was the synthesis route that led to the discovery of carbon nanotubes in 1991.[11] The carbon nanotubes produced via arc discharge are more crystalline and have fewer defect carbons than CNTs produced with other methods. The arc discharge method uses a cathode made of graphite and an anode containing a powdered carbon precursor and catalyst to synthesize carbon nanotubes in between the electrodes.[11] A current of 50-100 A is driven by a voltage of 20 V to produce high temperatures above 3000°C between the electrodes positioned 1 mm apart from each other.[10, 11] The carbon electrodes are usually encased in an inert gas with reduced pressure, but the procedure is tailored to create different configuration of fullerenes. The use of a flow gas containing hydrogen atoms instead of an inert atmosphere has been reported to synthesize CNTs more efficiently due to high reactivity of the hydrogen arc faces.[10] One of the advantages to using arc discharge is that the method is tunable to synthesize different types of CNTs. The manipulation of voltage applied changes the amount of residual catalytic metals present and the quality of CNTs produced. The diameter of the carbon nanotubes produced are highly affected by the temperature at which the CNTs were formed.[11] Arc discharge can also be modified to yield higher percentages of SWCNTs by tilting the cathode and anode by 30° or doping the graphite anode with catalytic metals.[10]

Chemical vapor deposition (CVD)

Chemical vapor deposition (CVD) is the most widely used method for synthesis of carbon nanotubes, largely due to the low production cost in comparison to other methods. During CVD, a layer of catalytic metal is used to grow the carbon nanotubes while inside of an oven.[12] This method uses temperatures around 700°C and a carbon containing flow gas to grow the carbon nanotube structure on the surface of the catalytic metals.

Since the catalysts used during synthesis are usually unknown to the buyer, the carbon nanotubes being studied have unknown catalytic impurities. The most common catalysts used are nickel, cobalt, and iron. The diameter of carbon nanotubes synthesized can be manipulated by differing size of metal particles.[10] Producers of industrial scale carbon nanotubes rarely disclose the type of catalytic metal or mixture of catalysts used as an effort to keep their product unique. Unfortunately, this keeps a variable about the carbon nanotube synthesis unknown to the public. These catalytic metals can be incorporated into the structure of the carbon nanotube as an impurity. These impurities can either be present on the outside wall of the carbon nanotube or be encapsulated within inner layers of the carbon nanotube. This method is also known to produce highly entangled bundles of CNTs that are hundreds of micrometers in dimension. In comparison to individual CNT structures, these bundles exhibit inferior mechanical and electrical properties.[13] This is due to lower aspect ratio and lower relative surface area that the CNT bundle has in contrast to if all of the CNTs were dispersed in the matrix. In comparison to other CNT synthesis methods, CVD produces carbon nanotubes with a lot of defect sites in the sp^2 hybridized carbon nanotube structure. These defects in the form of amorphous carbons, spherical fullerenes, and metal catalyst impurities negatively affect the observed properties of CNT reinforced composites.

Removal of metal impurities from the carbon nanotube structure is a difficult process that has not yet been perfected. The removal of an encapsulated metal impurity requires the use of an oxidative treatment to open the carbon shell while an unencapsulated impurity could be removed by washing with an acid. Both approaches damage the carbon nanotube's structure and therefore the unique properties that are created by the high concentration of sp^2 hybridized carbons.

While the presence of metal impurities affects the mechanical properties of carbon nanotubes, they also cause health problems to organisms that are exposed.[14] When carbon nanotubes are inhaled, they accumulate in the lungs and in different areas of the body if functionalized.[15] Over time, these carbon structures can partially degrade and release the metal impurity that was attached to the carbon nanotube structure. Once catalytic metals are released into the body, cytotoxicity of cells occurs which can lead to death. Some studies state that toxicity does not derive from carbon nanotubes themselves, but the catalysts that are so abundantly found in multi-walled carbon nanotube samples. While the toxicity mechanisms and routes of cytotoxicity in response to carbon nanotubes are still disputed, lung tumors have been observed in animal subjects exposed to carbon nanotubes.[14] The undisclosed knowledge of the catalysts used in the CNT synthesis method would be useful in determining the effect of catalyst impurities on cytotoxicity. Many biochemistry articles addressing CNT toxicity do not include information on catalyst impact since the mechanism of cytotoxicity is still disputed and the catalysts used are not a known variable anyways.

Laser ablation

Laser ablation is a technique that uses a high-powered laser to vaporize graphite in an inert atmosphere and collect the CNTs produced on a sample collector. The inert flow gas is used to move the vaporized carbon particles from the furnace to a water-cooled copper surface.[10] The technique is useful because highly pure multi-walled carbon nanotube structures can be produced with no catalytic impurities. The synthesis method is also tunable to create desired morphologies. The size and distribution of carbon nanotubes produced is dependent on the laser source, flow gas, and temperature of the furnace. When a small amount of catalytic metal is present on the target graphite, the method produces single walled carbon nanotubes.[10] While laser ablation can be used to synthesize a precise CNT structure with a low amount of impurities, it is not widely used industrially because of the high associated cost. Since it is so expensive, laser ablation is used mostly for single walled CNT synthesis for applications where consistent chirality is important.

1.3 CNT Properties

Single-walled carbon nanotubes (SWCNTs)

Carbon nanotubes are either single walled or multiwalled in their structure. Single walled carbon nanotubes can be classified as chiral, armchair, or zigzag conformations. The different configurations produce CNTs with different electrical characteristics. If the carbon bonds of a theoretical graphene sheet are aligned to be perpendicular to the x-axis and then rolled upwards, the resulting configuration would be zigzag. The diameter of SWCNTs ranges from about 0.4-3 nm. Carbon nanotube structures do not form below 0.4 nm because the curvature of the tube makes the structure thermodynamically unstable.[8]

As seen in Figure 2, the left point of the theoretical graphene sheet is always located at the origin (0,0). If the position of the right corner of the graphene sheet is moved off the x-axis, the resulting configuration will either be chiral or armchair. The annotation for the vector movement of the bottom right corner of theoretical graphene sheet is (n,m). If $n > m > 0$, the resulting configuration is chiral. If $n = m$, the CNT will have an armchair configuration.[16] For electrical material properties, the configuration of the carbon nanotubes is very important because armchair configurations produce CNTs with metallic properties with no bandgap. If the value of "$n - m$" is equal to a multiple of 3, then the CNT will have quasi-metallic properties due to its very small bandgap.[12] All other configurations are semiconducting due to their high bandgap. There are some exceptions to these configuration rules and their resulting characteristics due to CNT diameter. In applications of polymer chemistry, zigzag conformations of single walled carbon nanotubes have been found to produce composites with higher Young's modulus than armchair configurations.

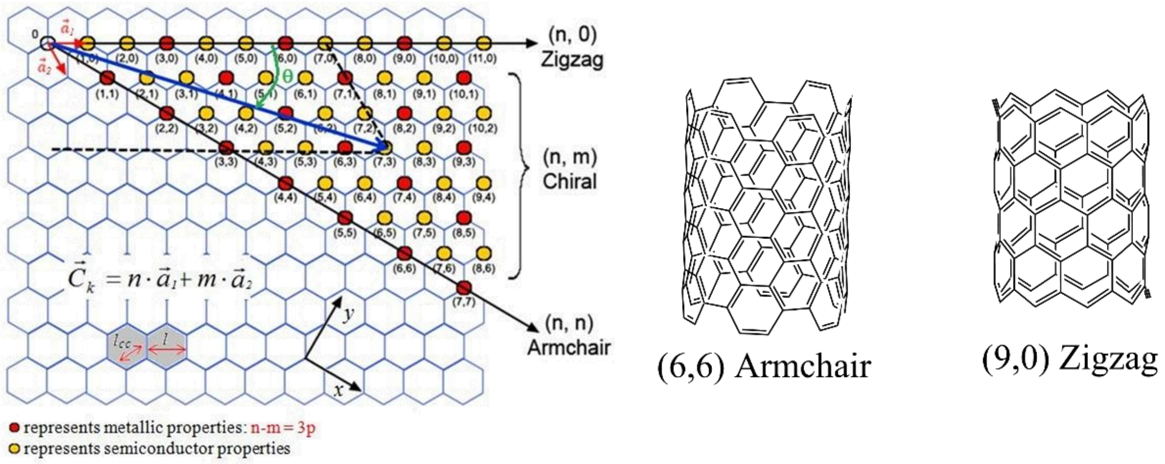

Figure 2. Chirality of carbon nanotubes and use of (n, m) vector values to determine configuration of carbon atoms. (Adapted from Attaf 2016)[17] Examples of armchair and zigzag CNT configurations are also displayed. (ChemDraw 2022)

When working with single walled carbon nanotubes, the configuration of the carbon atoms plays a large role in the characteristics that the resulting composite displays. When it comes to the actual production of SWCNTs, the resulting structure is nowhere near the theoretical "perfect" SWCNT model with all sp^2 hybridized carbon bonds; and therefore, neither the electrical nor mechanical properties of a "perfect" theorized SWCNTs are experimentally observed. The theoretical CNT structure of a SWCNT is a ballistic conductor, meaning its electron field emission promotes quantum tunneling of electrons.[18] Since the different configurations of carbon nanotube chirality are so similar in structure and formation energy, it is very difficult to obtain a consistent carbon nanotube chirality configuration with a conventional CNT production method like CVD.[19] In a perfect theoretical model of an armchair SWCNT, 100% of energy would conduct from one side of the nanotube through to the other side. Selective growth methods have been studied in recent years to synthesize carbon nanotubes with high precision of chirality properties within a sample, but this method is much more costly and not as easily scalable for industrial production yet.[19] This technology could be useful to improve current wiring systems, where a portion of the electricity is lost in transmission due to lack of full conduction of energy through the wires, referred to as transmission energy loss.[20]

Multi-walled carbon nanotubes (MWCNTs)

When working with multiwalled carbon nanotubes, there are multiple layers of carbon sheets that make the configuration of the carbon structures. These multiple layers of carbon make the overall chirality of CNTs less impactful towards the properties of MWCNTs in comparison to SWCNTs due to high probability of potential chirality configurations in each sample. Because of this, the theoretical chirality and configuration of the graphene sheets that make up the MWCNT structures have less research focus in literature in comparison to SWCNT. The theoretical model of MWCNTs has yet to be conclusively determined but it is generally believed that the outermost shell of carbon nanotube structures determines the generalized properties that the carbon nanotube will possess.

The two models of MWCNT are the multiple concentric tubes model and the parchment role model. In the multiple concentric tube model, multiple CNT structures of varying sizes are arranged inside of one another like Russian nesting dolls. In the parchment role model, the carbon nanotube structure is an induvial spiral of a graphene sheet rolled up like parchment paper.[10] In both models, the graphene layers would be around 3.4A apart from adjacent layers due to van der Waal interactions.[21] The diameter of the CNT along with functional groups can cause the interwall spacing to be manipulated to be closer or further apart. It has been determined that double-walled carbon nanotubes (DWCNTs) and MWCNT interlayer distances ranged from 2.7A to 4.2A.[22]

The study of double-walled carbon nanotubes (DWCNTs) has been a large contribution to the support of the concentric tube model because they can be seen via SEM to be composed of two separate single walled carbon nanotubes- one inside the other. As an example for chirality calculation complication, the DWCNT can be further studied. While the DWCNT has the fewest layers of any MWCNT, calculating the chirality of the two nanotubes that make up its structure is still quite difficult. For a CNT with diameter between 0.5-2 nm, there are hundreds of possible chirality's.[23] While the chiral structure of the outermost CNT can be analyzed with scanning tunneling microscopy (STM), it is a surface technique that can only probe the outer tube of the CNT. Transmission electron microscopy (TEM) can be further used to makes inferences about the innertubes diameter. If the inner-tuber diameter is determined to be in a range from 0.92 A to 1.38 A, that would leave 40 possible chirality configurations.[23] Further characterization based on metallic properties on the DWCNTs can reduce possibilities of the inner-tube chirality since the outer tube's chirality is known. Characterization of carbon nanotube structure becomes increasingly complicated as more walls are added to the CNT structure.

While research into CNT production has come a long way since their discovery, a method to consistently produce a certain configuration of nanotube at a reasonable price has yet to be commercially developed. Currently, when carbon nanotubes are purchased, chirality of CNTs is not even an aspect disclosed. The CNT producers regularly disclose the tube diameter and length, but in a range with a large percentage of error correlated to each value. Multiwalled carbon nanotubes are largely produced via CVD in which different manufacturers use different transition metals as their catalyst due to relative cost. The catalysts used by the manufacturer are not commonly disclosed and catalyst residues are commonly introduced into the CNT structure, creating defect sites. All these factors create confounding variables when producing and characterizing carbon nanotubes and CNT composites.

Carbon nanotubes have a theoretical tensile strength of 11- 100 GPa, which is nearly 100 times larger than that of steel.[24] It is difficult to determine tensile strength of such small structures, so composites are commonly produced with carbon nanotubes to be able to study the mechanical properties of the carbon nanotubes. Instrumentation like TGA, DSC, and DMA are commonly used to characterize properties of polymers and can be used to study the effect of CNTs on mechanical strength in composites.[25] These composites are useful on their own but can also be used to study the properties and structure of the carbon nanotubes.

Microwave Interactions

While the full mechanism for microwave and carbon nanotube interactions has yet to be fully agreed upon, there are two main mechanisms that can be used to explain the localized heating surrounding carbon nanotubes in the presence of microwave irradiation.

The first mechanism is based on the transverse parametric resonance due to the polarization of carbon nanotubes, which causes the electromagnetic energy from the microwaves to transform into mechanical vibrations.[26] This mechanism revolves around the use of carbons in the tangential plain of the CNT structure. The use of CNT-based composites with dielectric properties could be useful as high-performance microwave absorption materials.[27]

The second mechanism involves Joule heating of non-sp^2 hybridized carbons or other impurities due to the dampening of the transverse vibrational mode.[26] A research team from Beijing, China studied the addition of multiwalled carbon nanotubes and carbonyl iron nanoparticles into acrylic composite films before being exposed to microwave curing treatments. The carbon nanotubes were known to have large amounts of defect carbon sites so would absorb microwaves via Joule heating. The composites containing iron nanoparticles and defective MWCNTs produced films with improved microwave absorption. This study concluded that the electromagnetic match between dielectric MWCNTs and carbonyl iron nanoparticles.[28] This dielectric match is achieved by the presence of carbon stretching that is not tangential to the overall sp^2 hybridized CNT structure.

1.4 CNT Composites

The largest obstacle when creating composites with carbon nanotubes is the aggregation of the carbon nanotubes to one another. While the van der Waal interactions between the carbon structures are not particularly strong on their own, there are so many carbon nanotubes that have these van der Waal interactions that the accumulation of all of these weak intermolecular forces makes the CNTs to agglomerate together.[8] The van der Waal interactions observed in CNTs are due to the high specific surface area that CNTs possess.

A research team from India found that the addition of multiwall carbon nanotubes to acrylonitrile butadiene styrene (ABS) monomers increased mechanical and electrical properties of resulting composites. It was found that the tensile strength of composites peaked at 3 wt% MWCNT loading, the Young’s Modulus continued to increase as CNT loading was increased up to 10 wt% CNTs. The elongation sharply decreases up to 3 wt% CNT loading and then stays constant as CNT loading is increased. The tensile strength at 3 wt% MWCNT loading was 29% higher than that of ABS only polymers. The electrical conductivity of the composites are increased by the 7th order of magnitude to 10^{-5} Scm^{-1} with the addition of 10% MWCNTs.[25]

The interface between the carbon nanotube and the polymer matrix determines the mechanical properties of the composite. If there is no interaction between the CNT and the matrix, then the resulting composites is unable to transfer load which creates a brittle composite with low mechanical properties. The theoretical surface of unfunctionalized carbon nanotubes is a smooth, non-reactive sheet of carbon that cannot interact with the polymer matrix.[13] Functional groups can be added to the outside of the CNT structure to increase ability of the carbon nanotube to interfacial bond to polymer chains. When the interfacial strength between the CNT and polymer matrix is enhanced, the composite has an improved load transfer to the CNTs and therefore produces a stronger product.[24] When the carbon nanotube is functionalized with a covalent bond, photon transfer between carbon nanotubes and the polymer matrix is introduced which improves the thermal conductivity of the composite. Chemical functionalization methods with acidic treatment methods have been found to disrupt bonding between graphene sheets and decrease the buckling force of the carbon nanotubes by 15%.[29]

When epoxy nanocomposites with chemically functionalized CNTs, the electrical conductivity was drastically decreased due to the unbalanced polarization effect and the shortening of the carbon nanotube length.[30] While the electrical conductivity of polymers is an important aspect in specialty polymers, the more crucial deformation is the decrease in the CNT aspect ratio when acidic modifications are made. When the aspect ratio of the carbon nanotube decreases, the potential mechanical properties of the structure are diminished which is a large downside to acid-based functionalization methods. Functional groups can be added without damaging the CNT structure via covalent functionalization methods to allow for interfacial interactions to occur between the CNTs and matrix when creating composites. This interaction creates a homogeneous solution throughout the polymerization process and allows for optimal mechanical properties in nanocomposites.

A research team from Georgia Southern University (DiCesare et al 2013) previously functionalized carbon nanotubes with phenylmagnesium and styrenylmagnesium bromides.[31] The functionalized CNTs were then introduced in varying amounts to styrene polymer matrixes. It was concluded that the modulus and strength of the composites increases as the concentration of functionalized CNTs is increased. It was also calculated that the addition of 0.1 wt% functionalized CNTs led to a 4% increase in the Young's modulus.[31]

Dielectric Properties

Nanocomposites containing carbon nanotubes have been researched for their dielectric properties for applications in electronics. The dielectric constant is a quantitative measurement of how well a material stores electrical energy in an electromagnetic field while dielectric loss is the energy from the electromagnetic field that is not stored. Both attributes are important for electronic materials, especially for the use in rechargeable battery electrodes. While a "perfect" SWCNT structure is a ballistic conductor that would have amazing electrical capabilities, carbon nanotubes consistently have imperfections in their structure that make them have high dielectric loss.[18] Polymer composites containing CNTs are usually conductive and not considered dielectric materials because their dielectric loss is so large.[32]

While composites with high dielectric loss are not valuable for the transportation of electrons in electronic applications, polymer composites with high dielectric loss can be useful for precautionary or purposeful absorption and dissipation of excess high-wavelength energy in micro-technology.[33] While high-wavelength energy sources like EMPs interferes with electronic circuits, the use of electromagnetic absorption and shielding with MWCNT composites could be a preventative mechanism for military grade vehicle electronics. Wavelengths in the gigahertz frequency are becoming more prevalent with the progressive use of 5G networks.[27]

Multi-walled CNTs are found to have better electromagnetic shielding properties than that of SWCNTs and the increase of CNT loading increases the shielding efficiency.[33] A research team from Beijing, China published a paper showing that the introduction of functionalized MWCNTs with polypyrrole largely enhanced the dielectric performance of the composites while also ensuring good dispersion of the MWCNTs in the polystyrene matrixes.[32] Another research team investigated the effect of metal alloy functional groups attached to CNTs and their effect on the dielectric constant observed in polyurethane composites at a range of frequencies. The dielectric constant increased as the degree of functionalization of CNT with metal functional groups increases.[34] The dielectric properties of CNT composites will continue to be a studied topic; but, without improved CNT synthesis methods to produce more pristine CNT structures, the theoretical opportunities that CNTs propose will not be experimentally observed due to loss of energy because the structure is not actually a ballistic conductor.

CHAPTER 2

FUNCTIONALIZATION OF CARBON NANOTUBES

2.1 CNT Samples

Different manufacturers of carbon nanotubes use different methods and catalysts to produce their carbon nanotube product. These methods create a variety of different characteristics that effect how the carbon nanotubes absorb microwaves. Because of this, a variety of carbon nanotube sizes from different manufacturers were investigated. The type of carbon nanotube, the production company, and dimensions of the CNT structure can be found in Table 1 along with the date and type of functionalization group that the CNTs were manipulated to have. The manufacturers also publish a purity percentage that indicates what percentage of the carbon nanotubes produced are within the size dimensions reported. The Nanocyl company sells commercial grade carbon nanotubes labelled as “NC7000” that discloses no size dimensions or any other characterization information other than 100% pure. No further information about the carbon nanotube dimensions could be obtained after contacting the company. All CNT production methods used a catalyst in the chemical vapor deposition process, but the specific catalyst used is not disclosed publicly.

Table 1. Breakdown of CNT samples and known information

CNT Source	**CNT Type**	**Company**	**Outside Diameter (nm)**	**Length (μm)**	**Purity (wt%)**	**Functional Group**	**Functionalized CNT name**
A	MWCNT	Nanocyl	n/a	n/a	100	Styrenyl	s-funct (A)
B	MWCNT	Sigma Aldrich	7-15	0.5-200	95	Styrenyl Phenyl	s-funct (B) p-funct (B)
C	SWCNT	CheapTubes.com	1-2	5-30	60	Styrenyl	s-funct (C)
D	MWCNT	Sigma Aldrich	10-20	0.5-200	95	Styrenyl	s-funct (D)
E	MWCNT	CheapTubes.com	30-50	10-20	95	Styrenyl Phenyl	s-funct (E) p-funct (E)

2.2 Functionalization Strategy

To fully understand whether the addition of the styrenyl functional group to the carbon nanotubes is beneficial to the resulting composite, unfunctionalized CNTs and phenyl functionalized CNTs are also incorporated into composites to further study mechanical properties. Phenyl functional groups do not contain the conjugated double bond attached to the benzene ring that the styrenyl functional group has. To investigate hypothesized crosslinking starting at the carbon nanotube, the mechanical properties of phenyl-functionalized composite are studied and compared to those of styrenyl-functionalized CNT composites. Calculations were done to synthesize a 0.2M Grignard reagent capable of functionalizing 2% of the carbons in the carbon nanotube structure. Our target of 2% functionalization is due to attempting to add useful functional groups that can interact with the polymer matrix, but not so many that increased van der Waal interactions could induce agglomeration of carbon nanotubes.

2.3 Styrenyl Functionalization of CNTs

Grignard Reagent Synthesis

To functionalize the carbon nanotubes with a styrenyl functional group, a Grignard reagent is used. Styrenylmagnesium bromide (4-vinylphenylmagnesium bromide) was synthesized using a static nitrogen line to reduce exposure of the Grignard reagent to air.

A mortar and pestle are used to grind magnesium pellets to create maximum amount of surface area. Approximately 50mg of ground-up magnesium and a stir bar are dried under vacuum at 70°C overnight. The glassware that will be used to synthesize the Grignard reagent is placed in a convection oven at 110°C overnight.

The next day, 40.5mg of magnesium is weighed out and placed into a 100mL 3-neck round bottom flask. The dried stir bar is added to the 3-neck round bottom flask and two of the opening are sealed with pierceable tops. A two-way glass valve is attached to the open neck of the round bottom flask and fastened with a keck clamp. A vacuum is pulled through the two-way glass valve while the 3-neck round bottom flask is placed in an oil bath at 70°C for an hour to further dry the contents of the Grignard reaction flask: magnesium and stir bar. A schematic of the preparation for 1M Grignard reagent is displayed in Figure 3.

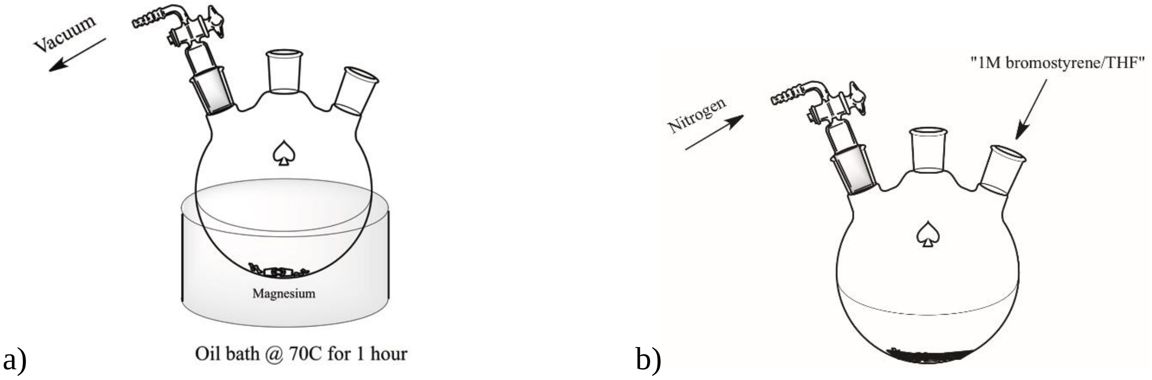

Figure 3. The first steps of preparing the Grignard reagent are a) further drying of the reaction chamber, magnesium, and stir bar along with b) the initiation of the Grignard reagent with 1M bromostyrene. (ChemDraw)

The two scintillation vials that were dried overnight are sealed with pierceable tops and labelled “1M bromostyrene/THF” and “THF only”. Using a glass syringe, 0.21mL of bromostyrene is added to the “1M bromostyrene/THF” vial. Using a different glass syringe, 1.45mL of THF is added to the “1M bromostyrene/THF” vial and 6.64mL of THF is added to the “THF only” vial. The 3-neck round bottom flask is removed from the oil bath and allowed to cool. The vacuum that is being supplied via needle is replaced with a static nitrogen line through the same pierceable top.

Approximately 25% of the “1M bromostyrene/THF” is added dropwise to the 3-neck round bottom flask containing magnesium and the rest of the vial’s contents are added a few minutes. This creates a 1M Grignard reagent to initialize the reaction while the static nitrogen line is still attached.

A 70°C mineral oil bath is prepared, and the static nitrogen line is removed. One of the pierceable tops of the 3-neck round bottom flask is replaced with a water-cooled reflux condenser before being placed into the oil bath. After the system begins to reflux, the contents of the “THF” vial are added via glass syringe in 1mL increments. The system is allowed to reflux for 1 hour. The preparation and reflux of the 0.2M Grignard reagent can be further visualized in Figure 4. The result of this process is 8.3mL of a 0.2M styrenylmagnesium bromide. The first step in Figure 5 shows the preparation of the Grignard reagent, which is the first step in functionalizing carbon nanotubes with styrenyl-functional groups.

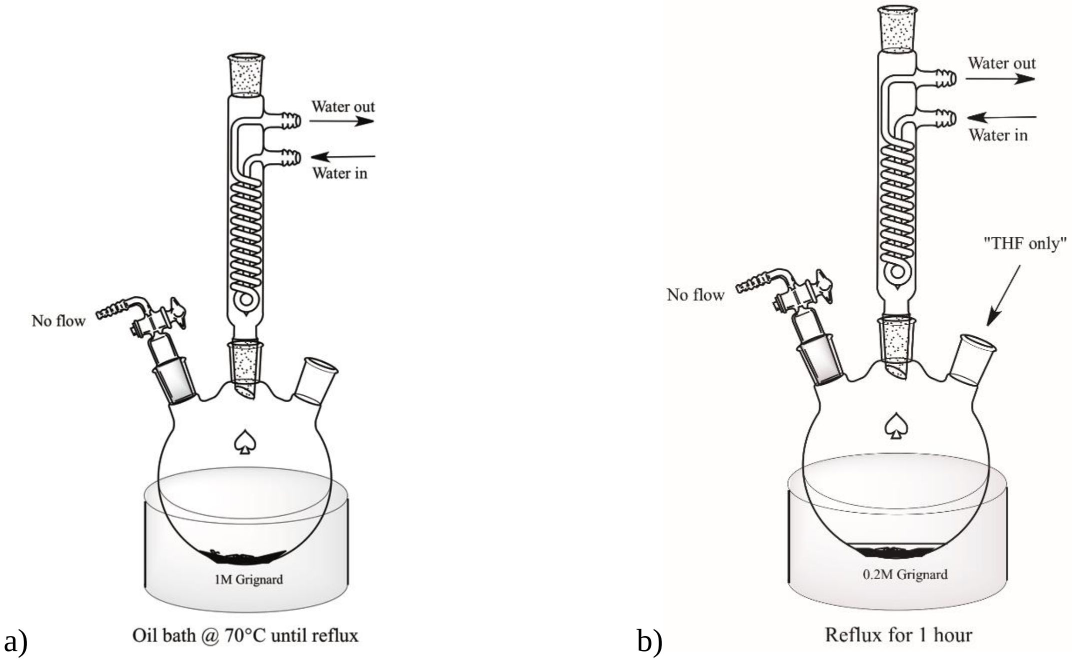

Figure 4. The final steps of the Grignard synthesis are a) initializing reflux with 1M Grignard solution before b) refluxing the 0.2M Grignard solution for 1 hour. (ChemDraw)

Grignard reagent calculations:

1M initial Grignard (1.66mL):

$$\left(\frac{1g\ CNTs}{1}\right)\left(\frac{0.02}{1}\right)\left(\frac{1\ mol}{12g}\right)\left(\frac{1mol\ Mg}{1\ mol\ C}\right)\left(\frac{24.305g}{1\ mol}\right) = \mathbf{0.04051}\boldsymbol{g\ magnesium}$$

$$\text{1.66mL Grignard}\left(\frac{\text{1L}}{\text{1000mL}}\right)\left(\frac{\text{1mol Grignard}}{\text{L}}\right)\left(\frac{\text{1 mol bromostyrene}}{\text{1mol Grignard}}\right)\ldots$$

$$\left(\frac{\text{183.04g bromostyrene}}{\text{1 mol}}\right)\left(\frac{\text{1ml}}{\text{1.46g}}\right) = \mathbf{0.208mL\ bromostyrene}$$

$$\text{1.66mL total} - \text{0.208mL bromostyrene} = \mathbf{1.452mL\ THF}$$

0.2M bromostyrene (8.3mL):

$$(\text{1.66mL})(\text{1M}) = (x)(\text{0.2M}) \text{ and } x = \text{8.3mL total solution}$$

$$\text{8.30mL(total volume)} - \text{1.452mL(initial THF)} - \text{0.208mL(bromostyrene)} = \mathbf{6.64mL\ THF}$$

The carbon nanotubes are covered with a Kimwipe and rubber band before being placed into a vacuum oven at 90°C overnight. This prevents any carbon nanotubes from escaping while repressurizing the vacuum oven compartment but allows for moisture to escape. Since Grignard reagents are extremely sensitive to moisture, the 500mL round bottom flask that will contain the functionalization process is placed into a convection oven at 110°C overnight.

The following day, the carbon nanotubes are removed from the vacuum oven and one gram is weighed out. This one gram of carbon nanotubes is added to the dried 500mL round bottom flask before a pierceable top is used to seal the round bottom flask. To prepare the carbon nanotubes to be functionalized, they must be suspended in a solvent that will not interact with covalent carbon bonds of the carbon nanotubes and will not induce agglomeration of the CNTs. Tetrahydrofuran is used to suspend the CNTs in the functionalization process because it satisfies both conditions. Approximately 200mL of THF is added to the 500mL round bottom flask. A vacuum is pulled followed by introduction of nitrogen through a static nitrogen line 3 times to expel any air that is in the 500mL round bottom flask. The 500mL round bottom flask is then bath sonicated for 2 hours while the Grignard reagent is being synthesized.

Once the 8.3mL of 0.2M styrenylmagnesium bromide is synthesized, a glass syringe is used to transfer the Grignard reagent into the 500mL round bottom flask containing the carbon nanotubes. Bath sonication of the 500mL round bottom flask is continued for one hour to allow Grignard reagent to encounter as many carbon nanotubes as possible. The first step of Figure 5 shows the synthesis of styrenylmagnesium bromide, the Grignard reagent for styrenyl-functionalization. The use of the Grignard reagent to functionalize one gram of carbon nanotubes can be seen in the second step of Figure 5.

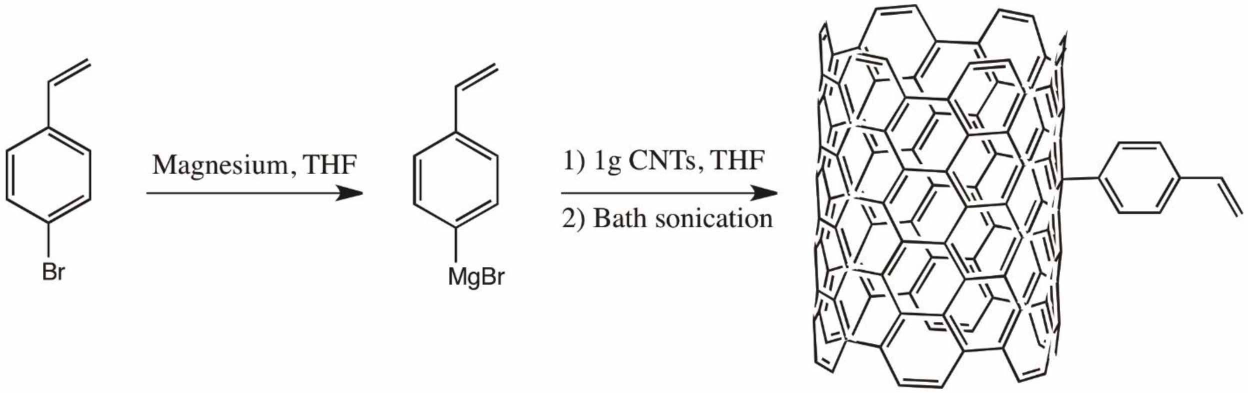

Figure 5. Styrenyl functionalization of carbon nanotubes with a synthesized styrenylmagnesium bromide Grignard reagent. (ChemDraw)

2.4 Phenyl functionalization of CNTs

To functionalize carbon nanotubes to have phenyl functional groups, phenylmagnesium bromide is used. Phenylmagnesium bromide is a much more commonly used Grignard reagent than styrenylmagnesium bromide so it could be purchased from Sigma Aldrich instead of being synthesized in our lab. To prepare for the functionalization of carbon nanotubes, the CNTs are covered with a Kimwipe and rubber band before being dried at 90°C overnight in a vacuum oven. A 500mL round bottom flask is placed in a convection oven at 110°C overnight.

The following day, one gram of carbon nanotubes is weighed out and added to the dried 500mL round bottom flask before being sealed with a pierceable top. A glass syringe is used to transfer 200mL of THF to the 500mL round bottom flask. The flask containing carbon nanotubes and THF is bath sonicated for 1 hour with a static nitrogen line before 0.6mL of 3M phenylmagnesium bromide is added dropwise via glass syringe. The 500mL round bottom flask is placed into a heated sonication bath for two hours with a static nitrogen line at 52°C. Figure 6 shows a schematic of the phenyl-functionalization of CNTs with a phenylmagnesium bromide Grignard reagent.

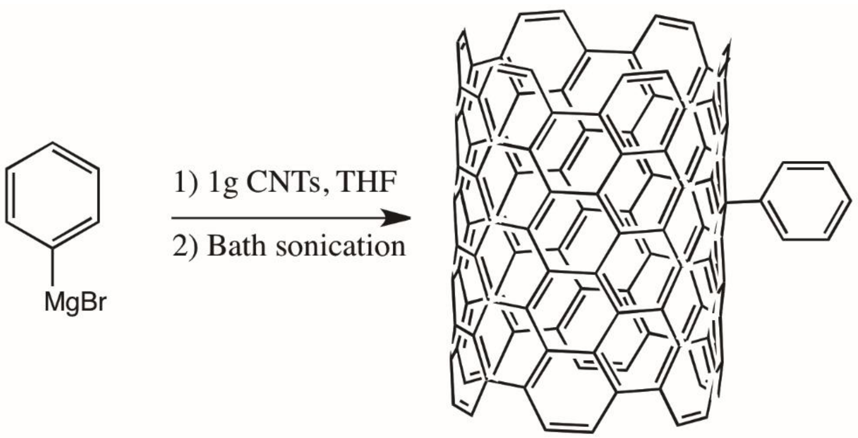

Figure 6. Phenyl functionalization of carbon nanotubes with purchased Grignard reagent. (ChemDraw)

Phenyl functionalization CNT calculations:

1M Grignard for 2% of carbons (stock= 3M phenylmagnesium bromide):

$$1.0\text{g CNTs}\left(\frac{1\text{mol}}{12\text{g carbon}}\right)\left(\frac{2}{100}\right)\left(\frac{1\text{mol Grignard}}{1\text{mol CNTs}}\right)\left(\frac{1\text{L}}{3\text{mol Grignard}}\right)\left(\frac{1000\text{mL}}{1\text{L}}\right)$$

$$= \mathbf{0.556mL\ phenylmagnesium\ bromide}$$

In both phenyl and styrenyl functionalization processes, one gram of unfunctionalized CNTs are bath sonicated in 200mL of THF. Figure 7 further displays how the CNTs are bath sonicated for two hours before being functionalized with a 0.2M Grignard reagent while suspended in THF solvent. Phenylmagnesium bromide and styenylmagnesium bromide Grignard reagents are used to phenyl and styrenyl-functionalize the CNTs respectfully.

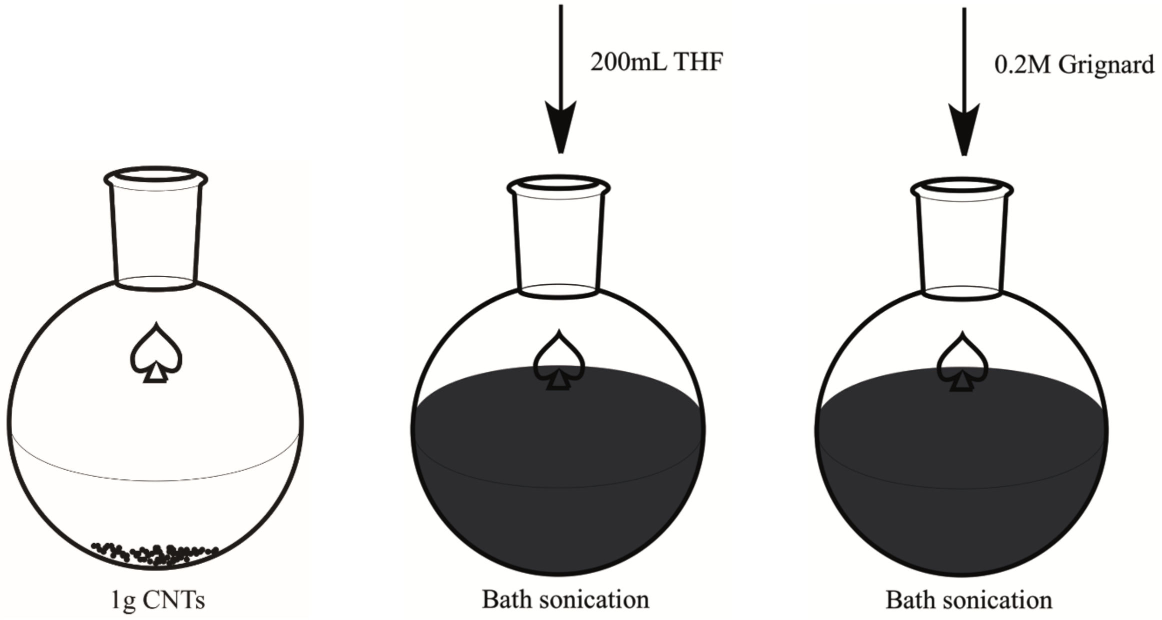

Figure 7. CNTs functionalized with 0.2M Grignard reagent. (ChemDraw)

2.5 Washing Functionalized CNTs

Once the functionalized carbon nanotubes have been sonicated in THF, the solution is washed via vacuum filtration to isolate the carbon nanotubes and remove any metal residues left over from the Grignard reagent. A glass vacuum filtration funnel is used to pull solvents through a Teflon filter with a vacuum pump. This glass vacuum filter holder is used to allow carbon nanotubes to saturate in the wash solution in between each solution used. Once the 200mL of THF and CNTs from the 500mL round bottom flask have filtered through the vacuum funnel, the carbon nanotubes are washed with five 20mL solutions:

The diluted solutions are prepared with deionized water and the filtrate is stirred occasionally during each wash step. The filtrate is also saturated with the following solution before the carbon nanotubes are dry enough to form cracks on the surface. This is done to reduce pathways for solvent to travel through the filtrate and increase interactions of all carbon nanotubes to the wash solutions. The filtrate is then transferred to a 20mL scintillation vial and dried at 90°C under vacuum overnight. Figure 8 shows the CNT washing procedure in which the R group signifies that the functional group does not change during the washing procedure and that both phenyl and styrenyl- functionalized CNTs are washed with this procedure.

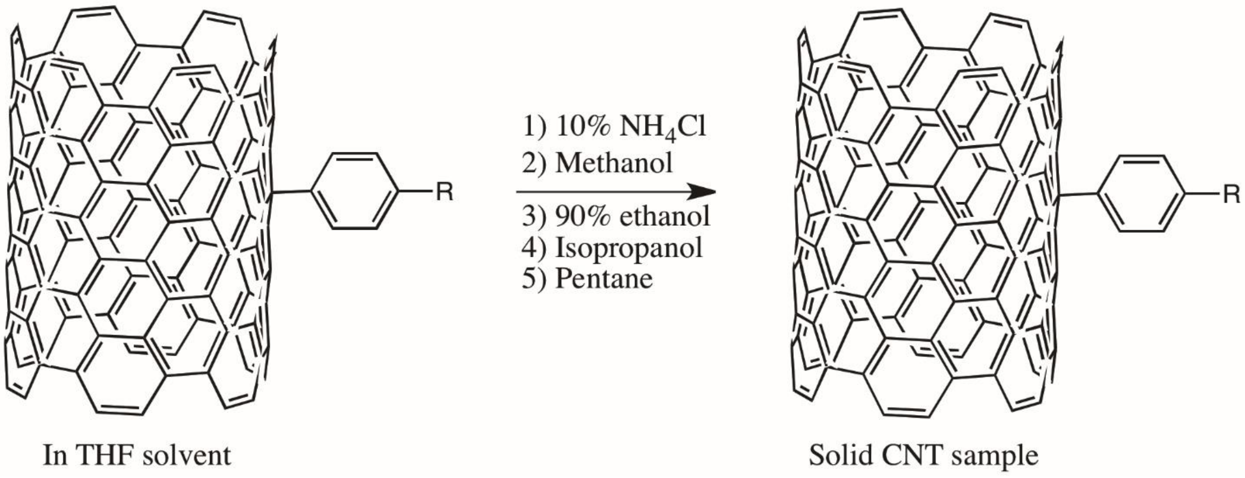

Figure 8. Functionalized carbon nanotube washing procedure. (ChemDraw)

Carbon nanotubes absorb moisture as soon as they are exposed to air. Because of this, the functionalized and functionalized carbon nanotubes in our lab are stored in a desiccator. To further remove moisture from the carbon nanotube samples, the carbon nanotubes that are stored in 20mL scintillation vials are covered with a Kimwipe fastened with a rubber band before being placed in a vacuum oven. The Kimwipe allows for moisture and organic solvents to escape but prevents the loss of carbon nanotubes. The sample is heated at 90°C under vacuum pulled from the house vacuum line overnight as a standard drying procedure. This drying procedure is used before all carbon nanotube characterization (Raman, TGA, and settling tests) and to dry the carbon nanotubes the night before functionalization and after functionalization.

CHAPTER 3

CNT CHARACTERIZATION

The unfunctionalized and functionalized carbon nanotubes are characterized using settling tests, thermogravimetric analysis (TGA), and Raman spectroscopy. These characterization tests are crucial to determining if functionalization was successful and how the manipulated carbon nanotubes differ from their unfunctionalized counterparts. All carbon nanotube samples were dried overnight via standard drying procedure before characterization to reduce confounding variables that moisture might produce in the collected data.

3.1 Settling Tests

To determine how well the carbon nanotubes suspend in a styrene matrix, dried carbon nanotubes are placed into 20mL scintillation vials with styrene to determine how long it takes for them to agglomerate after being placed in a bath sonication. The longer the carbon nanotubes stay in suspension, the more likely those carbon nanotubes and functional groups are to have a useful interface with the styrene matrix. The CNT and styrene solution is prepared at 0.20% and 0.22% by weight of carbon nanotubes. The CNT and styrene solution is bath sonicated for 10 minutes and pictures of the solutions are taken after 1min, 5min, 15min, 30min, 1hour, 3hours, and an extended time later. The settling tests of CNTs that are incorporated into styrene composites are displayed in Figure 9 while carbon nanotube samples that were not incorporated into composites in this research are shown in Figure 10.

Sample	CNT wt%	After 5 minutes	After 1 hour	After 3 hours
Nanocyl (A)	0.200%	 Virgin (A) S-funct (A)	 Virgin (A) S-funct (A)	 Virgin (A) S-funct (A)
CheapTubes (E)	0.200%	 Virgin (E) P-funct (E) S-funct (E)	 Virgin (E) P-funct (E) S-funct (E)	 Virgin (E) P-funct (E) S-funct (E)

Figure 9. Settling tests of unfunctionalized and functionalized Sample (A) and Sample (E) CNTs.

Sample/ date	CNT wt%	After 5 minutes	After 1 hour	Extended time later
SigmaAldrich (B) 7-15 nm	0.22%	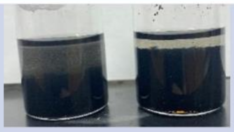 Virgin (B) S-funct (B)	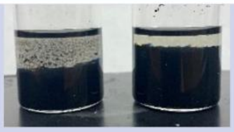 Virgin (B) S-funct (B)	5 days: 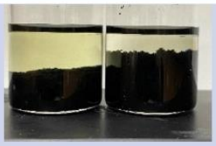 Virgin (B) S-funct (B)
SWCNTs (C)	0.22%	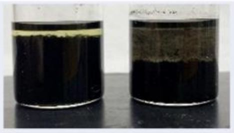 Virgin (C) S-funct (C)	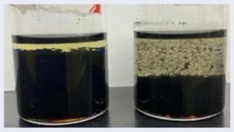 Virgin (C) S-funct (C)	45 days: 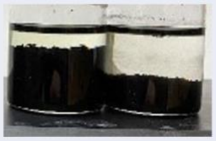 Virgin (C) S-funct (C)
SigmaAldrich (D) 10-20 nm	0.22%	 Virgin (D) S-funct (D)	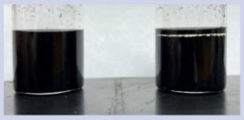 Virgin (D) S-funct (D)	3 days: 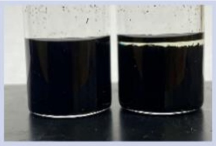 Virgin (D) S-funct (D)

Figure 10. Settling tests of CNT samples that were not selected for polystyrene/CNT composites.

The settling tests of CNTs, Figures 9 and 10, show how some CNTs tend to stay in suspension while some readily agglomerate. The carbon nanotubes in Figure 9 were incorporated into polymer composites due to their interface interactions with styrene observed in settling tests. The carbon nanotubes that tended to aggregate were not chosen to incorporate into a polymer matrix because aggregation of CNTs leads to reduced mechanical properties. If there is not a compatible interface interaction between the CNTs and styrene matrix, potential crosslinking would not be possible.

Settling test calculations:

20mg CNT and 20mL styrene solution:

$$20\text{mL styrene} * \frac{0.909\text{g}}{1\text{mL}} = 18.18\text{g styrene}$$

$$\frac{0.020\text{g CNTs}}{18.18\text{g styrene} + 0.020\text{g CNTs}} * 100 = \mathbf{0.110\%wt\ CNTs}$$

20mg CNT and 10mL styrene solution:

$$10\text{mL styrene} * \frac{0.909\text{g}}{1\text{mL}} = 9.09\text{g styrene}$$

$$\frac{0.020\text{g CNTs}}{9.09\text{g styrene} + 0.020\text{g CNTs}} * 100 = \mathbf{0.220\%wt\ CNTs}$$

30mg CNT and 16.5mL styrene solution:

$$16.5\text{mL styrene} * \frac{0.909\text{g}}{1\text{mL}} = 15.0\text{g styrene}$$

$$\frac{0.030\text{g CNTs}}{15.0\text{g styrene} + 0.030\text{g CNTs}} * 100 = \mathbf{0.200\%wt\ CNTs}$$

3.2 Thermogravimetric Analysis

A TA Instruments TGA Q50 is used for all thermogravimetric data collection. Thermogravimetric analysis is used to determine if functional groups have been added to the sides of the carbon nanotubes. This is done by recording the weight of the carbon nanotubes as they decompose in a nitrogen atmosphere. Since there is no air coming in contact with the sample, combustion is not a concern to confound data. The TGA instrument is set to have a flow rate of 20mL/min to the furnace and the balance. The TGA heating procedure is a 10°C/min ramp to 600°C. Thermogravimetric analysis data of unfunctionalized "virgin" CNTs and functionalized CNTs are displayed in Figure 11 to show the addition of functional groups to CNT structures.

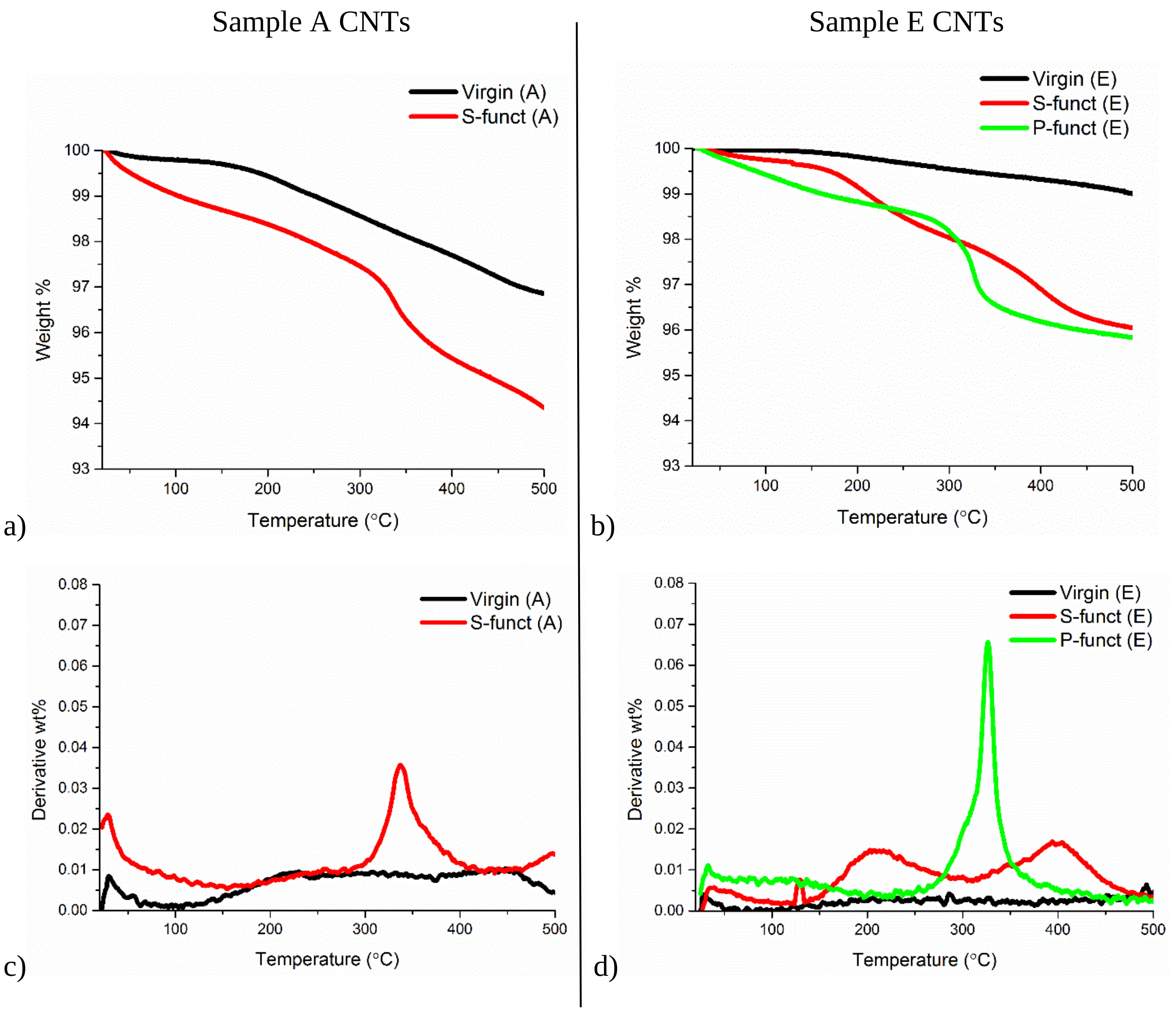

Figure 11. TGA of unfunctionalized and functionalized CNTs. Fig a) and c) show TGA data for Sample A CNTs and Fig. b) and d) show weight percentage and derivative weight percentage for Sample E CNTs.

The degradation of unfunctionalized carbon nanotubes differs between types of carbon nanotubes. It can be seen in Figure 11 that unfunctionalized Sample A CNTs degrade consistently between 200 and 450°C while the unfunctionalized Sample E CNTs degrade less than 1 wt% by the time the furnace reaches 500°C. Because of this discrepancy between CNT producers, the derivative wt% data comparison between unfunctionalized and functionalized CNTs is the most useful data analytics process. A peak in derivative wt% loss data shows the accelerated loss of mass at a specific temperature. This increase in derivative wt% loss correlates to the degradation of an attached functional group while the sp^2 hybridized bonds of the CNT are fixed carbons that would not readily degrade at temperatures below 500°C. All functionalized CNTs have an increase in mass loss. The s-funct A and p-funct E CNTs have a peak in derivative weight loss around 330°C. The s-funct E CNT sample has two regions of increased rate of degradation located at 200 and 400°C. A possible explanation for this is the presence of unattached styrenyl functional groups left on the CNT surface during functionalization. Another possible explanation is the functionalization of amorphous carbon in Sample A CNTs.

3.3 Raman Spectroscopy

A ThermoScientific DXR Raman Microscope with a 532 nm DXR laser is used for all Raman spectroscopy data collection. Raman spectroscopy is used to determine the ratio of disordered carbons there are in a sample of carbon nanotubes. Aromatic carbons show vibrational stretching in the G-band. Carbons that are sp^3 hybridized give vibrational stretching in the D-band. The ratio between the area of these integrated peak can be used to determine if more defect carbons are present in samples of carbon nanotube.

Dried carbon nanotubes are smeared onto a glass slide with a spatula. A 532nm laser is used with 4mW of power and a 50nm slit opening. Each spectra collected is the sum of 64 scans. Seven spectra were collected on different areas of the carbon nanotubes. The peaks of all seven of the spectra were integrated and the average ratio between the D-band and G-band are displayed in in Figure 12. The D-band represents defect carbon stretching; so, as the ratio increases, the higher percentage of defect carbon vibrations are found in the carbon nanotube. The G-band is located around 1575 cm^{-1} and the D-band is located around 1350 cm^{-1}.

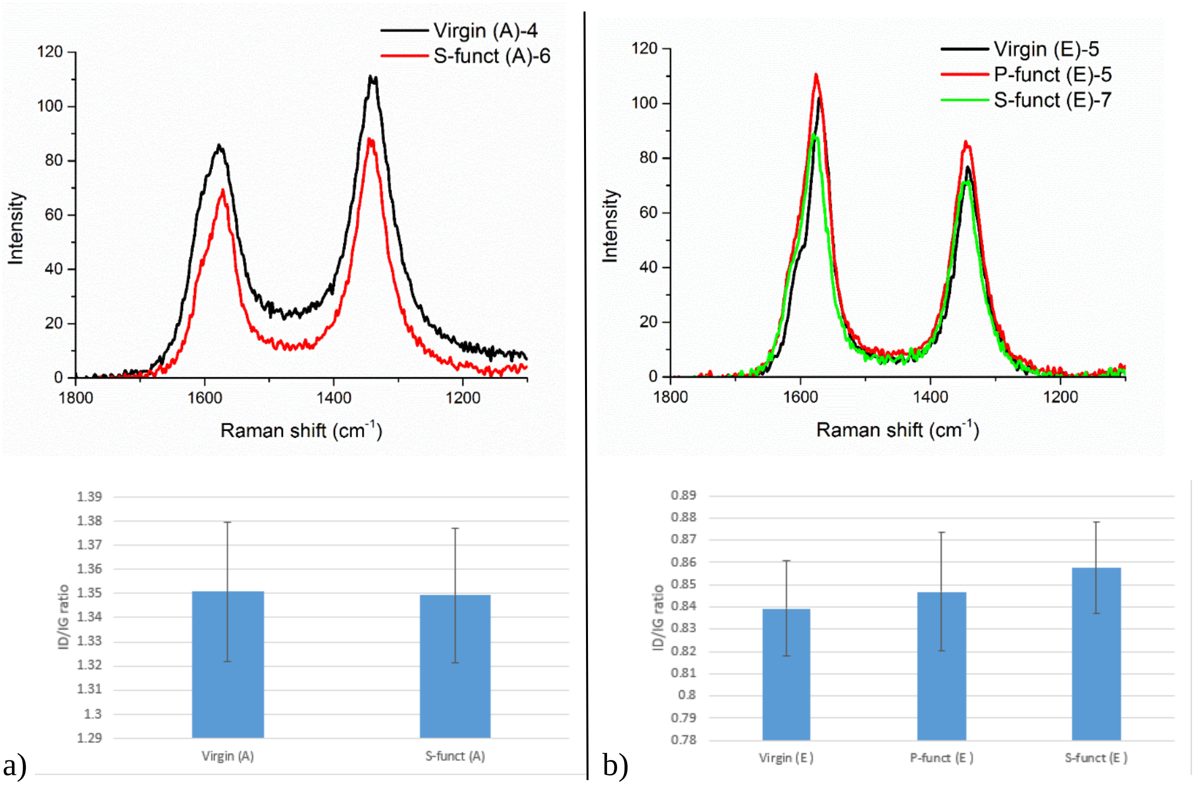

a) b)

Figure 12. Raman spectroscopy peak integration to calculate defect carbon ratio.

As seen in Figure 12, the integrated area ratio between the D and G-band does not show a statistically significant difference when comparing unfunctionalized and functionalized CNTs from the same manufacturer. Because of this, Raman spectroscopy cannot be used to determine if functionalization of carbon nanotubes was successful based on data collected from Raman spectroscopy alone. Target functionalization of the CNT samples was a maximum of 2% by weight. Since such a small amount of the carbons are targeted for functionalization, the analysis method is not precise enough to determine successful or unsuccessful functionalization. It is also seen in literature that the interactions between layers of multiwalled carbon nanotubes produce a variation of low frequency carbon stretching that complicate Raman spectroscopy data explanations.[23] The average ratio between the integrated areas of the D and G-band along with the standard deviation are plotted in Figure 13 for both Sample A and Sample E CNTs.

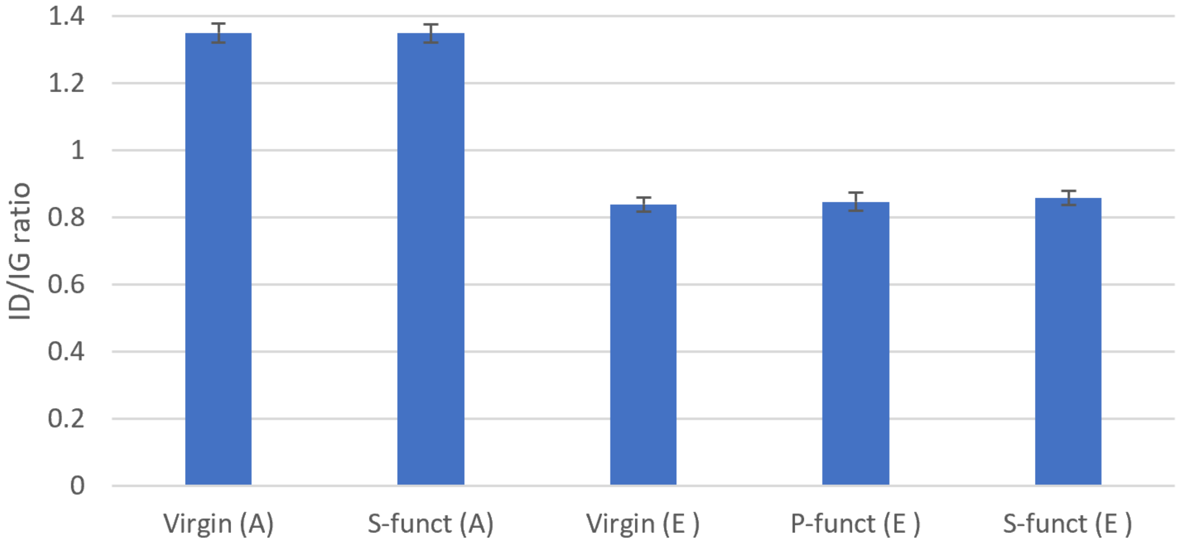

Figure 13. The ratio between integrated areas of D and G band from Raman spectroscopy are calculated and graphed along with the standard deviation.

The differentiation of CNT manufacturer has a larger impact on the defect carbon ratio than functionalization of carbon nanotubes. Sample A CNTs have a higher ratio of defect carbon stretching in comparison to the Sample E CNTs. The presence of amorphous and defect carbon sites produces more localized heating around the CNT due to the Joule heating mechanism when CNTs interact with microwaves.[26] The increased presence of defect carbons decreases the potential for the CNT to exhibit enhanced mechanical properties when incorporated into polymer matrixes.

3.4 Conclusion

Settling tests concluded that Sample A CNTs have better interfacial interactions with the styrene matrix than the other CNTs investigated. The interfacial interactions between CNTs and styrene monomer give a glimpse into how CNTs will agglomerate during the polymerization process. The aggregation of reinforcers in the styrene matrix will lead to reduced mechanical properties. Thermogravimetric analysis can be used to observe degradation of functional groups under a nitrogen atmosphere. This shows that some functional groups were added to the CNT structure, but not to the extent of 2% of the carbon content. Derivative weight percentage data from the TGA can also be used to see amorphous carbons present in Nanocycle CNTs before and after functionalization processes. Raman spectroscopy data further shows the increased defect carbon concentration that is present in Sample A CNTs in comparison to Sample E CNTs. The differentiation between unfunctionalized and functionalized CNTs could not be detected with statistical significance with Raman spectroscopy data.

CHAPTER 4

POLYSTYRENE/CNT COMPOSITES

4.1 Composite Sample Preparation

Due to data collected from settling tests, Raman spectroscopy, and thermogravimetric analysis; it was determined that the best carbon nanotubes to produce composites with were carbon nanotube samples A and E from Table 1. Further information about this decision can be found in Chapter 3.

A breakdown of the created composites can be found in Table 2. Composites are made with unfunctionalized CNTs and included in characterization data to compare composite strength characteristics against functionalized CNTs. Unfunctionalized carbon nanotubes are referred to as “virgin” CNTs and therefore composites made with unfunctionalized CNTs will commonly be referred to as “virgin CNTs composites”.

Table 2. The polystyrene/CNT composites synthesized for characterization. All composites have 0.1%wt CNT loading.

Composite Name	Power Source	Polymerization Time	CNT Sample	Functional Group
Styrene comp (oven)	Convection oven	10 hrs @ 130°C	-	-
Virgin A comp (oven)	Convection oven	10 hrs @ 130°C	A	-
S-funct A comp (oven)	Convection oven	10 hrs @ 130°C	A	Styrenyl
*S-funct A w/BPO comp (oven)	Convection oven	10 hrs @ 130°C	A	Styrenyl
P-funct E comp (oven)	Convection oven	10 hrs @ 130°C	E	Phenyl
S-funct E comp (oven)	Convection oven	10 hrs @ 130°C	E	Styrenyl
Styrene comp (MW)	Microwave/ Convection oven	8 min @ 200W 10 hrs @ 130°C	-	-
Virgin A comp (MW)	Microwave/ Convection oven	8 min @ 200W 10 hrs @ 130°C	A	-
S-funct A comp (MW)	Microwave/ Convection oven	8 min @ 200W 10 hrs @ 130°C	A	Styrenyl
*S-funct A w/BPO comp (MW)	Microwave/ Convection oven	8 min @ 200W 10 hrs @ 130°C	A	Styrenyl
P-funct E comp (MW)	Microwave/ Convection oven	8 min @ 200W 10 hrs @ 130°C	E	Phenyl
S-funct E comp (MW)	Microwave/ Convection oven	8 min @ 200W 10 hrs @ 130°C	E	Styrenyl

*Composite contains 5%wt benzoyl peroxide (free radical initiator)

To prepare 5g polystyrene/CNT composites, 5mg of CNTs and 5.5mL of styrene are added to a dry scintillation vial or microwave test tube. The calculations to synthesize 5g composites containing 0.1% CNT by weight are displayed below. The composite is then cured in the convection oven only or with a microwave pre-cure treatment that can be seen in Table 2. Composite samples were originally made with 5 grams of styrene and then later scaled up to produce 15g composites for further composite characterization testing.

5g composite calculations:

- 5.5mL styrene
- 5mg CNTs
- 0.25g BPO (if applicable)

$$5.5\text{mL styrene}\left(\frac{0.909\text{g}}{\text{mL}}\right) = 5.00\text{g styrene}$$

CNT/Styrene Composites (0.1% wt CNT):

$$\frac{0.0050\text{ g CNT}}{5.00\text{g styrene} + 0.0050\text{g CNT}} * 100 = \mathbf{0.0999\%\ CNT}\text{ (by weight)}$$

Free Radical Initiator Composites (5% wt BPO):

$$\frac{0.250\text{g BPO}}{5.00\text{g styrene} + 0.0050\text{g CNT} + 0.250\text{g BPO}} * 100 = \mathbf{4.76\%\ BPO}\text{ (by weight)}$$

$$\frac{0.0050\text{g CNT}}{5.00\text{g styrene} + 0.0050\text{g CNT} + 0.250\text{g BPO}} * 100 = \mathbf{0.0951\%\ CNT}\text{ (by weight)}$$

4.2 Benzoyl Peroxide

To further study the initiation step of polymerization, free radical initiators are added to some composites. Once free radicals are added to the polymer matrix, propagation of the polymer chain begins and monomers are step-wisely added to the growing polymer chains.

A CEM Discovery microwave was used to prepare composites because the temperature and pressure inside the vial can be monitored during polymerization with this instrument. The high spike in PSI associated with AIBN polymerization initiation is concerning when using a closed system microwave like the CEM Discovery microwave, so the use of this free radical initiator was not further used to produce composites.

Benzoyl peroxide is a commonly used free radical initiator that works similarly to AIBN but does not produce nitrogen as a byproduct. Because of this, BPO was used in two composites to determine how the addition of free radical initiators effects the mechanical properties of the composite. In Figure 14, the major product from BPO decomposition is the benzoyl radical in the middle which initiates polymerization with the free radical present on the oxygen atom. A minor product is a benzene rings with a free radical and a small amount of CO_2 but no statistically significant rise in PSI was observed during microwave polymerization with BPO. This further decomposition is a minor product because aromatic rings with free radicals are highly unstable.

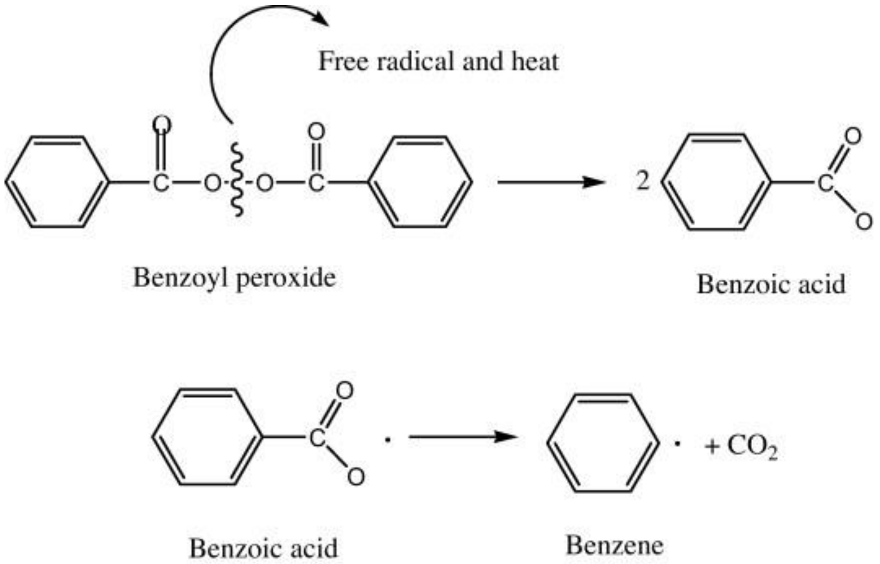

Figure 14. Mechanism for how heat breaks benzoyl peroxide down into a free radical initiator. (Adapted from Liu et al. 2015)[35]

Two composites that contained 5% by weight of BPO were created and characterized in comparison the composites that had no free radical initiators added. These composites are denoted in table 2 and are included in the collection of characterized composites to further study the initiation potential of functionalized carbon nanotubes.

4.3 Convection Oven Only Polymerization

Polymer composites are made with 0.1% CNT loading by weight. The calculations for carbon nanotubes, styrene, and free radical initiators can be found in Chapter 5.1 and a breakdown of the carbon nanotubes used in each composite can be found in Table 2. The day before the composites are made, the carbon nanotubes are dried under vacuum at 90°C overnight via standard drying procedure and six 10mL-scintillation vials are placed in a convection oven at 110°C to dry the glassware.

The Kimwipe and rubber band are removed from the vial containing dried carbon nanotubes and 5mg of carbon nanotubes is added to a dried scintillation vial before being sealed with a screw-on top. Each scintillation vial is labelled with a sticker and 5.5mL of styrene is added to each vial before being re-sealed with the screw-on top. All of the composites along with a scintillation vial with only 5.5mL styrene are bath sonicated for 30 minutes before being placed in a convection oven that has been preheated to 130°C for 10 hours.

The 5g composites are synthesized in 10mL-scintillation vials and microwaveable test tubes. To remove the composite, the glass vial is placed into a plastic bag and wrapped in a paper towel before carefully being hit with a hammer to remove all glass. Once all glass has been removed from the composite, the polymer is put into another plastic bag and broken with a hammer into small pieces.

4.4 Microwave/ thermal post-cure Polymerization

Carbon nanotubes are dried via standard drying procedure and six microwavable test tubes are placed in a 110°C convection oven to dry overnight. The dried carbon nanotubes are removed from the vacuum oven and 5mg of designated carbon nanotube is placed into a dried microwaveable test tube before being labelled and sealed with pressure releasing caps designed for the CEM Discovery microwave. Styrene is measured out using a graduated cylinder and 5.5mL is added to each of the microwaveable test tube before being resealed with the cap. The cap is replaced after every new addition to limit moisture in the vial and to reduce carbon nanotube loss due to the vacuum hood. All 5 composites and a microwaveable test tube with styrene only are bath sonicated for 30 minutes at room temperature. Each test tube is then microwaved for a total of 8 minutes at 200 W. The microwave is programmed to stop microwave production when the temperature of the solution reaches 120°C. Due to the physical characteristics of the carbon nanotube structures, the composites heated at different rates which required different microwave radiation treatments.

Composites containing Sample A CNTs reached the 120°C temperature threshold within the first minute of microwave radiation. Because of this, the solution was microwaved until the temperature gauge reached 120°C and then allowed to reduce temperature and release pressure by the microwave instrument. The composite is taken out and the homogeneity of the solution is noted along with viscosity. The composite is then microwaved again at 200W until the sample reaches 120°C. The temperature and pressure are allowed to decrease before the instrument releases the sample. This cool down process usually takes about 2 minutes. The homogeneity and viscosity are again recorded, and this process is repeated until the final amount of microwave irradiation is equal to 8 minutes at 200W.

In contrast, composites containing Sample E CNTs do not reach 120°C after 8 minutes of constant 200W of microwave irradiation. Because of this, the microwave polymerization step for these samples is simply placing the composite in the microwave for 8 minutes at 200W to receive the same Joules of energy as their “oven only” composite counterparts. It can also be seen in Figure 15 that the absorption of microwave irradiation by different manufacturers of CNTs correlates to observed viscosity of the composite after a total of 8 minutes in the microwave at 200W.

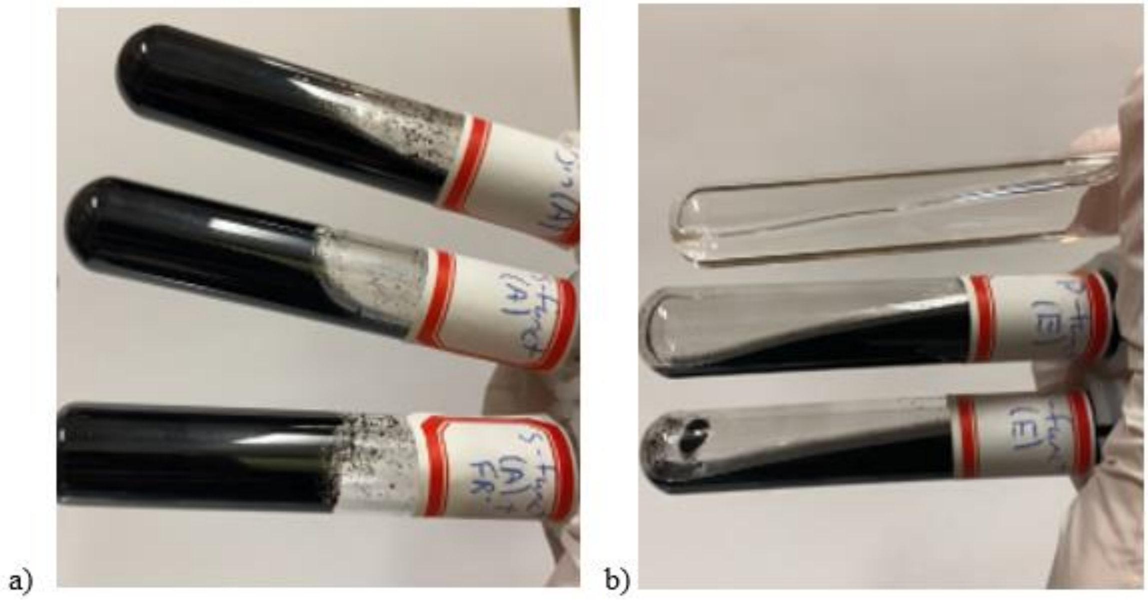

Figure 15. The viscosity of polystyrene/CNT composites after being microwaved at 200W for 8 minutes. a) virgin (A), s-funct (A), and s-funct (A) wBPO microwave composites. b) styrene, p-funct (E), and s-funct (E) microwave composites.

4.5 Scalable Polymerization

To create larger sample sizes for DMA and tensile strength testing, the same polymerization procedures are used but with samples three times as large. Since the CEM Discovery microwave can only irradiate samples 6mL and smaller, three 0.1% wt CNT solutions are prepared for each of the microwave composite samples and microwaved for 8 minutes at 200W in microwavable test tubes. The solution is then transferred from the test tube into a 20mL scintillation vial before being placed in the convection oven for 10 hours at 130°C. The oven only composites are prepared in 20mL scintillation vials with 15mg of carbon nanotubes and 16.5mL styrene to create 0.1% wt CNT composites. All composites are sealed for the 10 hour post-cure process.

15g composites calculations:

- 16.5mL styrene
- 15mg CNTs
- 0.75g BPO (if applicable)

$$16.5\text{mL styrene}\left(\frac{0.909\text{g}}{\text{mL}}\right)=15.00\text{g styrene}$$

CNT/Styrene Composites (0.1% wt CNT):

$$\frac{0.0150\text{ g CNT}}{15.00\text{g styrene}+0.0150\text{g CNT}}*100=\mathbf{0.0999\%\ CNT}\text{ (by weight)}$$

Free Radical Initiator Composites (5% wt BPO):

$$\frac{0.750\text{g BPO}}{15.00\text{g styrene}+0.0150\text{g CNT}+0.750\text{g BPO}}*100=\mathbf{4.76\%\ BPO}\text{ (by weight)}$$

$$\frac{0.0150\text{g CNT}}{15.00\text{g styrene}+0.0150\text{g CNT}+0.750\text{g BPO}}*100=\mathbf{0.0951\%\ CNT}\text{ (by weight)}$$

4.6 Composite Sample Molding

The duel heated platen hydraulic press is heated to 200°C. Once the platen reach 200°C, one metric ton of pressure is applied to the composite mold. As the composite material reaches its glass transition temperature, the pressure reading decreases. Hydraulic platen distance is decreased to continue a 1 metric ton of pressure until pressure is constant for 3 minutes. The hydraulic press heat source is turned off and allowed to cool for 10 minutes while pressure is still being applied. The water-cooling system is turned on for 5 minutes to allow mold plates to cool and composite to become solid again. The hydraulic press pressure is released, and the composite mold is removed from the plates. The composites are removed from the aluminum mold and polymer that had been pressed out of the edges was collected in a separate vial.

The 15g composites (large scale) are pressed into a thin sheet at 200°C before being placed into the polymer strip mold. This method reduces the potential of separation of agglomerated CNTs from styrene monomer and therefore produces samples with more homogeneity of CNTs and styrene. These samples were used for DMA and tensile strength testing due to greater dispersion of CNTs in the matrix and to keep data analysis consistent.

To create uniform pieces of composite for characterization testing, a hydraulic press with heating capabilities is used. The hydraulic press mold has a top and bottom plate to force polymer into the 4 shallow slots that make thin plastic composites. These plates are wrapped in aluminum foil and sprayed with Teflon non-stick spray. The mold is placed flush onto one of the aluminum foil-covered plates and small pieces of composite are placed into the mold's four slots. The other non-stick slate is placed on top of the mold and composite pieces and the system is placed into the hydraulic press with no pressure applied. The hydraulic press procedure using 5g composites can be seen in Figure 16.

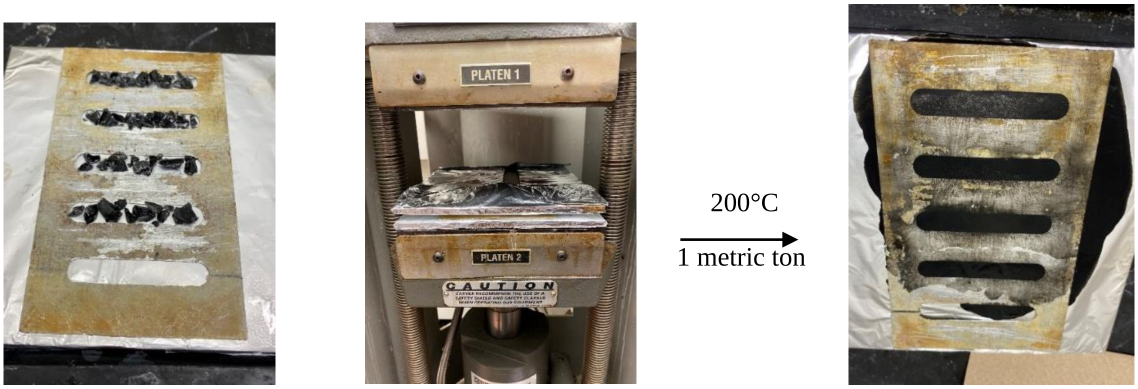

Figure 16. Composite preparation for characterization from 5g composites.

CHAPTER 5

COMPOSITE CHARACTERIZATION

To analyze consistently prepared composite samples, all samples characterized are small pieces that are broken off of the thin plastic composites that were formed in the hydraulic thermal press. Small pieces are used to increase the surface area of the composite being analyzed thermogravimetrically and to be able to fit into the small DSC pans. When the surface area is increased, more accurate data can be collected for characterization.

5.1 TGA

A TA Instruments TGA Q50 is used for all thermogravimetric data collection. The heating procedure is a 10°C/min ramp to 550°C with a flow of nitrogen gas at a rate of 20mL/min. Nitrogen is used as the flow gas so that the combustion of the carbon structure does not need to be accounted for. To clean the platinum pan, the flow gas is switched to air at the end of the TGA run and the temperature is ramped to 800°C at a rate of 20°C/min. TGA data is displayed as weight percentage of original mass at room temperature (Figure 17) and as the derivative of weight percentage (Figure 18) to study degradation trends of polystyrene/CNT composites.

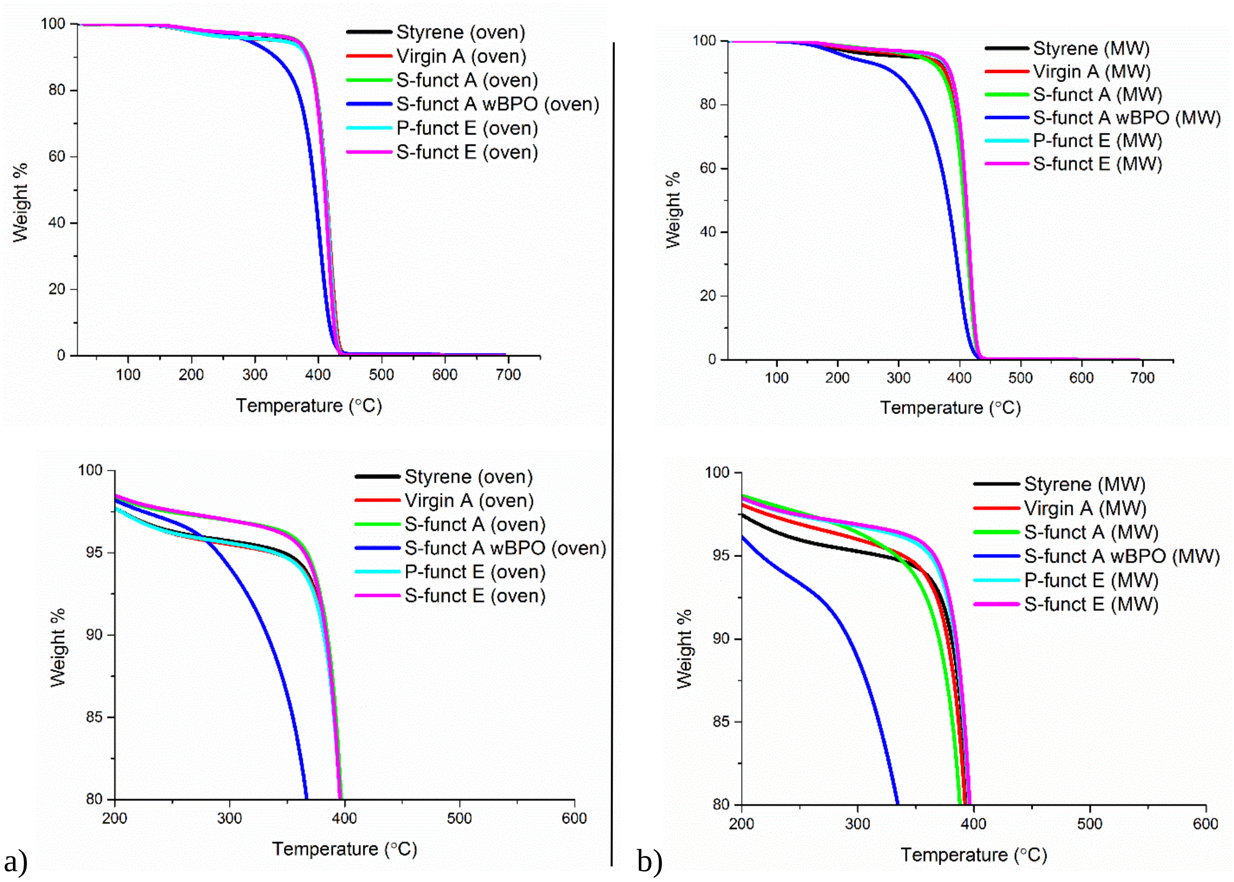

Figure 17. Thermogravimetric analysis data of a) oven only composites and b) microwave pre-cure composites. Zoomed in data is presented below graph of all data points.

In Figure 17a, the thermal degradation of oven only composites containing styrene, virgin A CNTs, and p-funct E CNTs are identical. Both composites containing styrenyl-functionalized CNTs retained a higher weight percentage than baseline styrene polymer and then had a similar degradation at 400°C. This retention of polymer chains at increased temperatures shows that the polymer has stronger bonds. This could show crosslinking or better packing of polymer chains.

In Figure 17b, the degradation of microwave composites shows a larger variety of degradation patterns. The styrene composite degradation appears to be the same for oven only and microwave composites. The styrenyl and phenyl functionalized Sample E CNT composites had a decrease in mass loss but a similar degradation trend in comparison to styrene composites.

The composites containing Sample A CNTs stayed at a higher weight percentage in comparison to styrene composites up until 350°C but sharply degrade as they reach 400°C. The exposure of microwave pre-cure treatments to polystyrene/CNT composites reduces the degradation rate of the composite when BPO is not present. The addition of styrene monomers to the CNT structure in the polymer matrix is a possible explanation for this trend but will need further characterization techniques to back-up this theory.

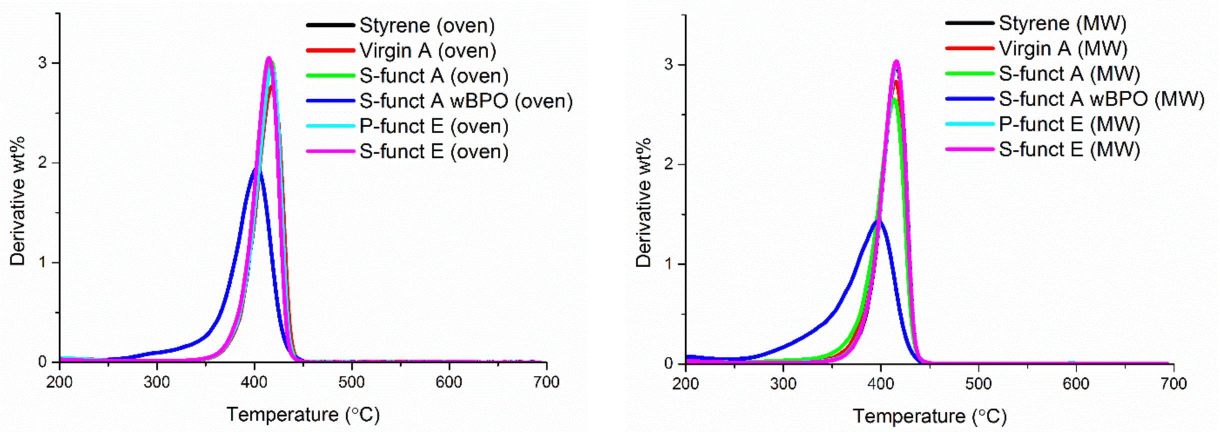

Figure 18. TGA data of all composites showing the derivative weight percentage.

The TGA data displaying derivative weight percentage as the y-axis for oven and microwave pre-cure composites, Figure 18, shows that composites containing benzoyl peroxide (BPO) degrade at lower temperatures than baseline styrene polymers or composites containing CNTs. It can also be seen in Figure 17 that oven and microwave composites containing free radical initiators degrade at temperatures much lower than other composites. The styrenyl-functionalized “E” CNT composites had elevated polymer chain retention in both oven and microwave composites.

5.2 DSC

A TA Instruments DSC250, discovery series with cooling chiller, is used to perform all DSC data collections. Hermetic pans are used to seal 8.0- 8.9 mg samples for all DSC data collection. To determine the glass transition temperature (T_g) of the produced polymers, DSC data collection is started at -20°C and ramped up to 260°C. The temperature is then decreased down to -20°C before increasing back up to 260°C to determine if the glass transition temperature of the polymer has changed. Differential scanning calorimetry is used to determine the phase changes of materials. Endothermic and exothermic reactions can also be detected if the polymer has not fully polymerized.

DSC data is collected using polymers that were made in 5g and 15g synthesis techniques. Two of the three analysis were completed using the 5g sample technique while one T_g value is derived from samples prepared using the 15g sample technique. Further information about the composite preparation and up-scale versions can be found in Chapter 5. DSC data collected from samples prepared using the 15g composite preparation technique are displayed in Figures 19 and 20. In Figure 19, the blue line shows the DSC data for the first ramp cycle while the red data shows the glass transition of the composite based on the second heating cycle. The second heating cycle is used to characterize composites and their T_g values. The first heating cycle is highly dependent on the thermal history of the polymer, so DSC data is routinely analyzed for T_g values based on the second heating cycle (Figure 20). The average T_g values derived from the second heating cycle of three DSC data collections are graphed in Figure 21 along with the standard deviation as error bars.

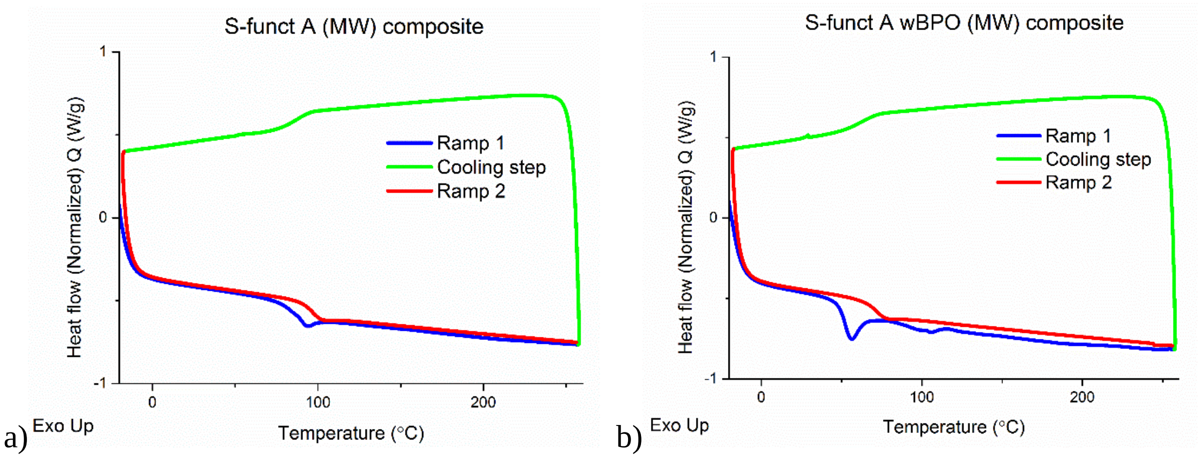

Figure 19. DSC data of a) S-funct A- microwave composite and b) S-funct A wBPO-microwave composite showing first and second ramp cycle.

The trends obtained from the first heating cycle in DSC can be used to further understand the distribution of polymer chain length. This can be used to see if the composite is fully polymerized or if the product is made up of multiple phases or different distinct polymer chain lengths. These trends are used to make inferences and to further explain other data, but cannot be used to calculate polymer chain length. During the first heating cycle, multiple glass transition temperatures can be seen in composites containing BPO. This data can be used to infer that the composite is made up of polymer chains of variant length. The drop in heat flow observed in the second heating cycle of DSC is always at a higher temperature than the first heating cycle. This can be explained by the overall packing of polymer chains once the polymer matrix gets above its glass transition temperature and then transitions back into a solid during the first heating and cool-down cycle.

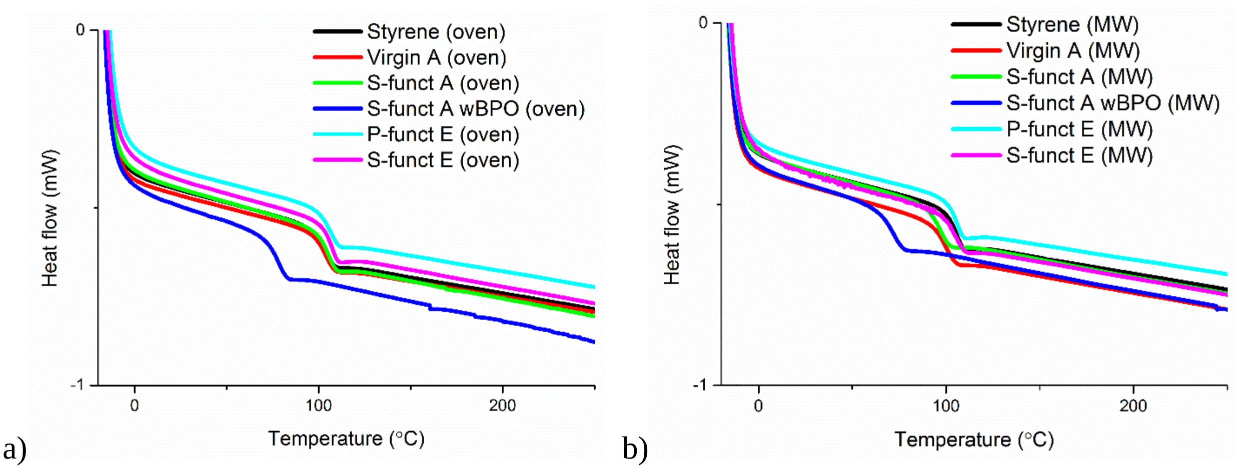

Figure 20. DSC data of second ramp cycle for all composites. a) Oven only composites and b) microwave pre-cure composites

When analyzing the T_g values obtained from the second heating cycle, the glass transition temperature of composites containing BPO is consistently lower than that of other composites due to polymer chain length shortening. This drop in T_g can be explained by the overall polymer chain shortening that occurs because of an increase in polymerization initiation sites. The average glass transition temperature values that are calculated from the second heating cycle of DSC are graphed in Figure 21.

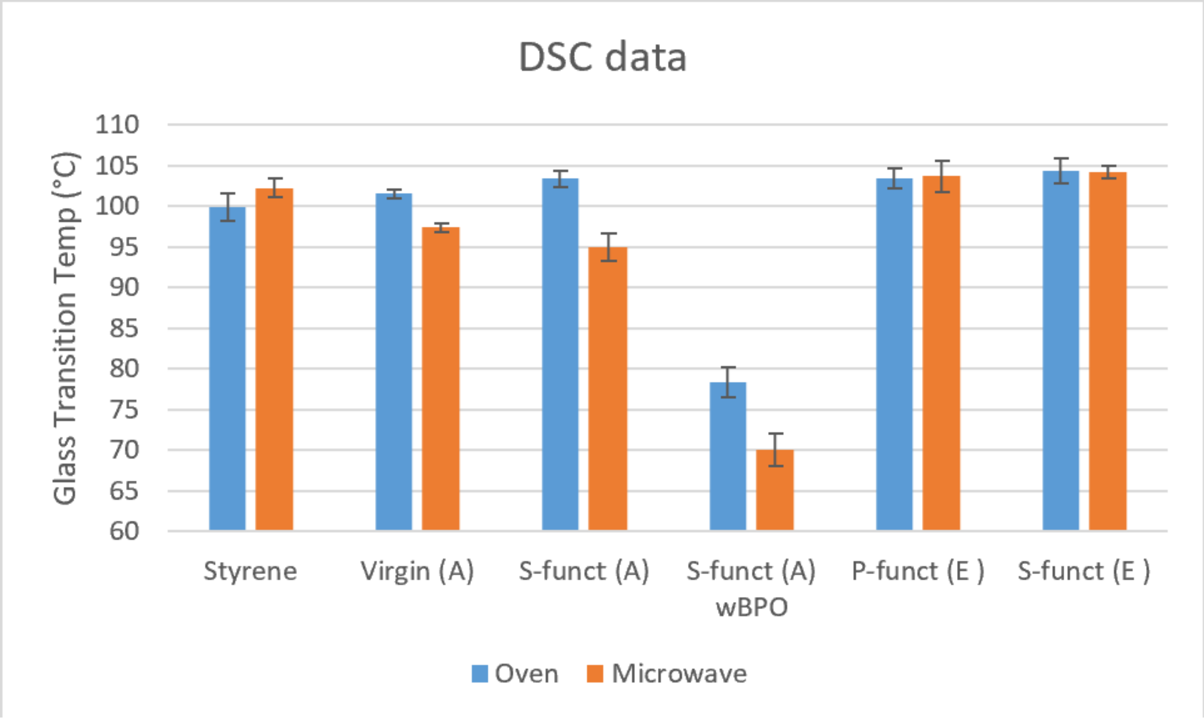

Figure 21. Reported T_g values obtained from second heating cycle of DSC data analysis. Data is derived from three DSC runs and standard deviation is also displayed.

Composites containing phenyl and styrenyl-functionalized E CNTs have a slightly elevated glass transition temperature in comparison to styrene polymers that do not have any carbon nanotubes (Figure 21). The addition of sample "A" CNTs to oven only composites leads to a slight increase in T_g while composites containing the same type of CNTs have a reduced T_g when exposed to a microwave pre-cure treatment. If BPO is added to the composite, the glass transition temperature decreases considerably due to shorter polymer chains in both oven-only and microwave pre-cure composites. The chain shorting of the composites containing BPO is amplified when the microwave pre-cure treatment is used since the average T_g of the microwave composite is considerably lower and statistically significant based on standard deviation calculations. Since the T_g of all microwave composites containing sample "A" CNTs had a reduced glass transition temperature, there is evidence that supports sample "A" CNTs have the ability to initiate polymerization, especially if they are functionalized with styrenyl functional groups.

5.3 X-Ray Diffraction

A PANalytical EMPYREAN XRD instrument with a Cu tube at 45kV and 40 mA is used to analyze all composites using X-Ray diffraction. X-Ray diffraction is used to study crystallinity of structures and polystyrene is generally viewed as an amorphous polymer. The samples are analyzed from 5 to 60 (2Θ) at 0.01° step sizes every half second. The scan speed is 0.02 °/sec and there are 5500 steps in each repetition. Every dataset graphed is the average of 10 repetitions.

Amorphous chains can still orient themselves into structured configurations by packing next to and on top of one another. This generalized structure of packed amorphous chains refracts X-Rays similarly to crystalline structured atoms at angles lower than 30° (2Θ). Because of this, the overall packing of polymer chains can be investigated with XRD (Figure 22). This packing of polymer chains can further be explained by pi-stacking of aromatic rings in polystyrene polymer chains.[36] One possible explanation for this could be the generalized orientation of styrene monomers induced by the microwave field before being further polymerized via heat.

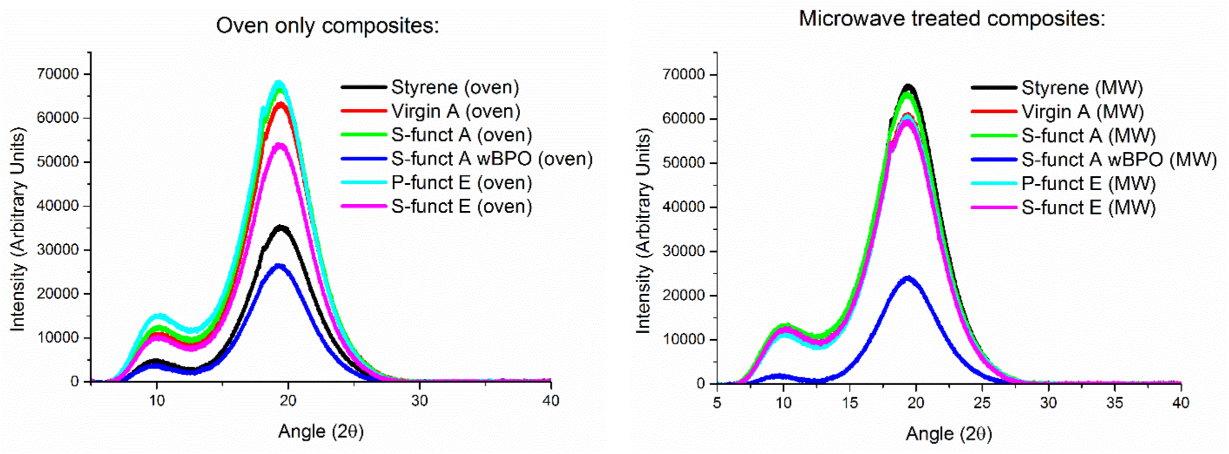

Figure 22. X-Ray diffraction data of oven only and microwave pre-cure composites.

In Figure 22, the ordered arrangement of composites containing a free radical initiator decrease in apparent crystallinity. This can be explained by the production of a lot of short polymer chains. These shorter polymer chains that contain benzoyl peroxide end groups create polymer chains that do not pack together as well.[37] The exposure to microwaves does not seems to affect the packing of polystyrene matrixes when benzoyl peroxide initiators are present. It should also be noted that the crystallinity of microwaved neat styrene appears to be just as structurally ordered as the composites containing carbon nanotubes in Figure 22.

5.4 DMA

Dynamic mechanical analysis is a widely used technique in polymer characterization that measures the ability of a composite to store energy elastically. All DMA data is collected using a TA Instruments DMA Q800 using a three-point bending techniques to test the viscoelastic properties of the polymer as a function of temperature.[38] Small sections of the thin composites are broken off to obtain square pieces. Sandpaper is used to create uniform, rectangular composites for DMA testing. A caliper is used to make sure the edges are completely flat and perpendicular to the other sides. The caliper is also used to measure the width and height of the composite. The composite widths ranged from 9mm to 10mm, the height ranged from 0.50mm to 0.70mm, and the length is a constant of 5mm due to the DMA clamp size. The procedure is a DMA multi-frequency strain test with a 3-point bending clamp. The DMA method uses an amplitude of 14.0µm with 0.020N of preload force and a force track of 125%. The instrument equilibrates to -60°C and then starts data collection. The temperature is ramped to 150°C at a rate of 3°C/min and then data collection is terminated. The storage modulus of the composite is recorded throughout the ramp procedure to determine the strength of the created polymers. Output data from DMA experiments shows the storage modulus and tan delta that can be used to determine glass transition temperature (Figure 23). Tan delta data uses storage modulus and loss modulus for its calculations, but storage modulus data can be used to visualize trends viscoelastic material deformation.

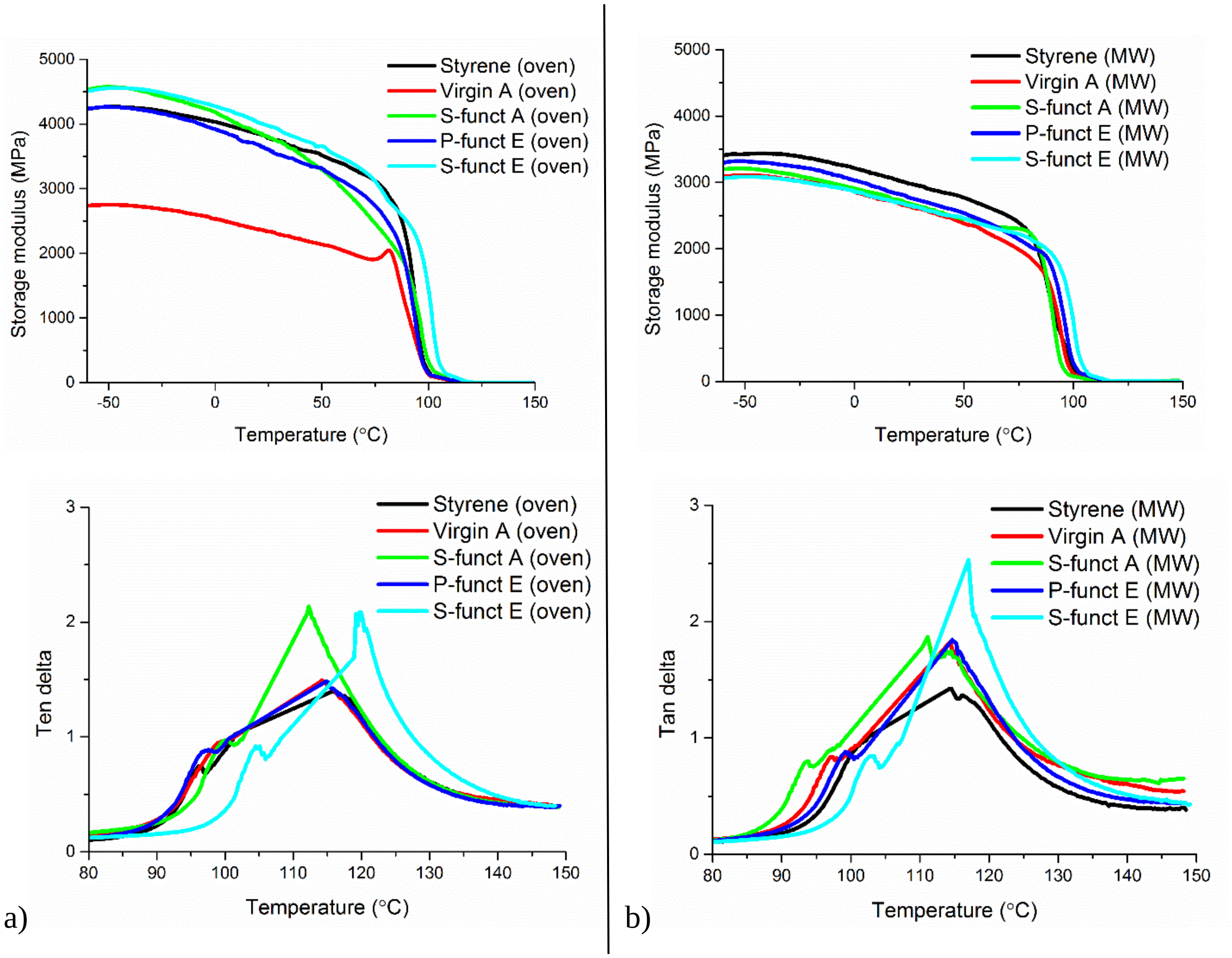

Figure 23. The DMA data of storage modulus and tan delta of storage modulus data are graphed for all composites. a) Oven only composites and b) Microwave pre-cure composites.

When analyzing DMA data, it should be noted that molecular weight of polymer chains has practically no effect on the storage modulus before the glass transition temperature (T_g).[39] The peak of the Tan delta data from Figure 23 can be used to determine the glass transition temperature. The glass transition temperature can be used to gain insights into extent of crosslinking. The more crosslinking that there is present in a polymer, the higher the T_g will be due to restricted molecular motion.[39] The glass transition temperature of each polymer composite is displayed in Figure 24 to further study the entanglements of polymer chains.

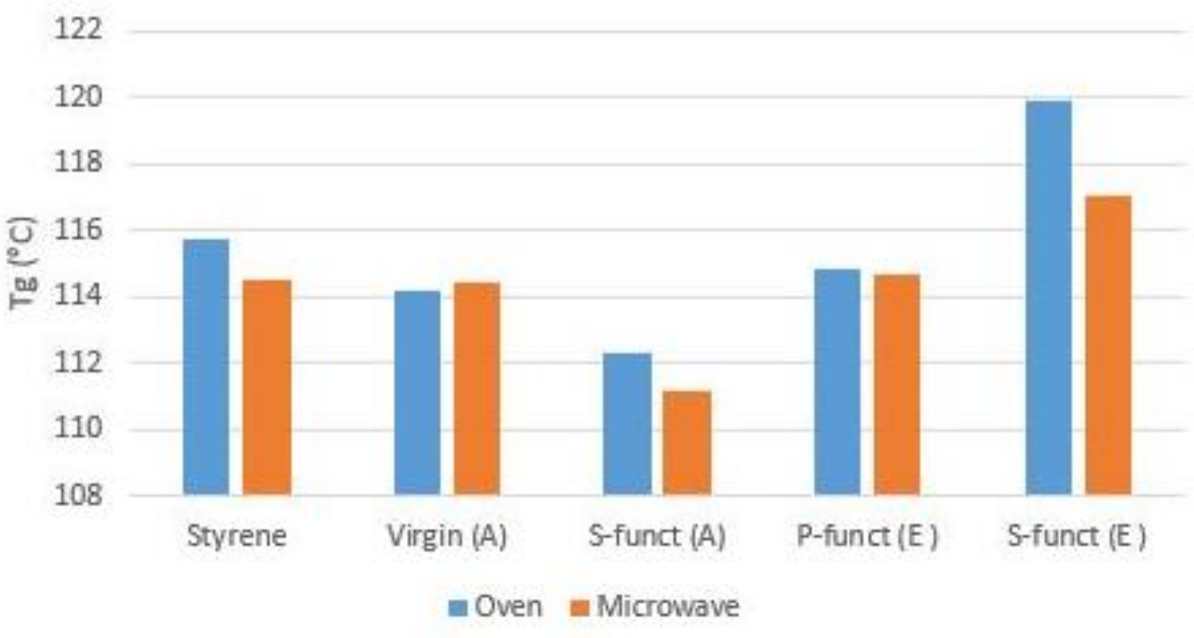

Figure 24. The T_g values derived from DMA data is graphed. Values are derived from tan delta peak from DMA data.

Figure 24 displays the effect of functionalized CNTs on the T_g of polystyrene/CNT composites. When comparing composites that were polymerized only in the oven and composites exposed to a pre-cure microwave treatment, the T_g appears to decrease slightly in neat styrene, s-funct A, and s-functionalized E composites. The glass transition temperature for composites containing unfunctionalized A and p-functionalized E CNTs are all the same.

The addition of s-functionalized A CNTs leads to a decrease in glass transition temperature and the addition of s-functionalized E CNTs leads to an increase in T_g. In both s-functionalized CNT composites, the addition of a pre-cure microwave step decreased the T_g. This shows that the type of carbon nanotube and styrenyl functional groups can be used to tune the mechanical properties of nanocomposites. The overall shift of glass transition temperature can be manipulated with the presence of defect carbons in the CNT structure. The use of microwave irradiation as a pre-cure treatment can be used to further understand the dielectric loss mechanism for explaining microwave interactions with carbon nanotube structures. Both explanations for microwave absorption, Joule heating and dielectric loss, can be further studied using the glass transition temperatures obtained from DMA data.

CHAPTER 6

CONCLUSION

When characterizing polystyrene/CNT composites, it is important to incorporate the data collected from multiple characterization techniques into a comprehensive explanation for the data. The mechanical properties of polystyrene/CNT composites are highly dependent upon the manufacturer of CNTs. This could be due to presence of amorphous carbon or residual catalysts left in the CNT bundles during CVD synthesis.

Joule heating from microwave interactions is centered around the presence of amorphous carbons and catalytic impurities. It is known through Raman spectroscopy and TGA that Sample A CNTs contain higher concentration of defect carbons and amorphous carbon impurities. Composites turn to a viscous solution after a pre-cure microwave step when Sample A CNTs are present due to extensive localized heating. This viscosity change also supports theory that polystyrene polymerization can be induced by a microwave field when carbon nanotubes are present in the matrix. While the interfacial interactions that Sample A CNTs have with styrene matrixes is superior to all other CNTs investigated in settling tests, their integration into polystyrene/CNT composites leads to lower glass transition temperatures. This reduction in T_g could infer polymer chain shortening, but there is no evidence of this seen in thermogravimetric analysis.

Polystyrene/CNT composites containing stryrenyl-functionalized E CNTs displayed increased glass transition temperatures from DSC and DMA characterization. Composites containing Sample E CNTs had an increased mass retention in thermogravimetric analysis. Sample E CNTs have a lower ratio of defect carbons as seen from Raman spectroscopy and TGA data. Since there is less amorphous carbons present, there is less Joule heating when the CNTs interact with microwaves. Since there is less localized heating, polymerization is not initiated from microwave interactions with Sample E CNTs and there is no viscosity change in the composite. When exposing Sample E CNT composites to microwaves, limited localized heating is observed, which makes the polymerization process safer and easier from a manufacturing standpoint.

XRD shows an increase in crystallinity for all polystyrene/CNT composites in comparison to baseline styrene prepared in the convection oven. This increase in XRD peak intensity is correlated to the stacking of pi bonds that refracts X-Rays. The microwave field is able to orient polymer chains into configurations of repeating pi-pi stacking to pack polymer chains together. This packing of polymer chains can also be used to further explain increased retention of mass in thermogravimetric analysis. The addition of benzoyl peroxide as a free radical initiator reduces the mechanical properties of all polystyrene/CNT composites that it was added to. The glass transition temperatures derived from DSC and DMA characterization techniques dropped drastically and the packing of polymer chains due to pi stacking is reduced when BPO is present. When free radical initiators are added to polymer matrixes, the polymer chain length is shortened due to increasing number of polymerization initiation sites.

The addition of functionalized CNTs reduces aggregation in composites. The mechanical properties of polystyrene/CNT composites are slightly altered with the presence of microwave pre-cure treatments. The effect of amorphous carbon in CNT structures and microwave absorption abilities can be further investigated with Sample A and Sample E CNTs.

Future work will investigate the impact of increasing the loading weight of carbon nanotubes in polymer composites. Only 0.1%wt CNT loading polymer composites were synthesized in this research. Up to 5%wt CNT loading should be used to observe the thermomechanical properties of polystyrene/CNT composites.

In future work, Sample E CNTs will be used to further investigate full-cure polymerization processes through microwave irradiation. Composites containing Sample A CNTs were not suitable for full microwave polymerization due to extreme localized heating at 200W. This led to the polymer matrix reaching boiling points within a minute due to Joule heating from amorphous carbons in the CNT sample. This rapid increase in temperature is too fast for industrial usage since it would be difficult to scale up a system that readily superheats in localized position in the polymer matrix.

Future work will also investigate pyrolysis processes induced with microwave irradiation for end-use plastic recycling. It is hypothesized that thermoplastics incorporated with CNTs could absorb high wattage microwave energy to break down the polymer chains for recycling.

REFERENCES

(1) DoH, N. Right to Know: Hazardous Substance Fact Sheet- Styrene Monomer. Health, N. J. D. o., Ed.; 2016.

(2) Jae Lee, W.; Froment, G. F. Ethylbenzene Dehydrogenation into Styrene: Kinetic Modeling and Reactor Simulation. *Industrial & Engineering Chemistry Research* **2008**, *47* (23), 9183-9194. DOI: 10.1021/ie071098u.

(3) Pantazis, D.; Chalari, I.; Hadjichristidis, N. Anionic Polymerization of Styrenic Macromonomers. *Macromolecules* **2003**, *36* (11), 3783-3785. DOI: 10.1021/ma025898m.

(4) Isac-García, J.; Dobado, J. A.; Calvo-Flores, F. G.; Martínez-García, H. Chapter 8 - Organic Synthesis Experiments. In *Experimental Organic Chemistry*, Isac-García, J., Dobado, J. A., Calvo-Flores, F. G., Martínez-García, H. Eds.; Academic Press, 2016; pp 239-289.

(5) Ramli Sulong, N. H.; Mustapa, S. A. S.; Abdul Rashid, M. K. Application of expanded polystyrene (EPS) in buildings and constructions: A review. *Journal of applied polymer science* **2019**, *136* (20), 47529. DOI: 10.1002/app.47529.

(6) Thakur, S.; Verma, A.; Sharma, B.; Chaudhary, J.; Tamulevicius, S.; Thakur, V. K. Recent developments in recycling of polystyrene based plastics. *Current Opinion in Green and Sustainable Chemistry* **2018**, *13*, 32-38. DOI: https://doi.org/10.1016/j.cogsc.2018.03.011.

(7) Bayda, S.; Adeel, M.; Tuccinardi, T.; Cordani, M.; Rizzolio, F. The History of Nanoscience and Nanotechnology: From Chemical-Physical Applications to Nanomedicine. *Molecules (Basel, Switzerland)* **2019**, *25* (1), 112. DOI: 10.3390/molecules25010112 PubMed.

(8) Atif, R.; Inam, F. Reasons and remedies for the agglomeration of multilayered graphene and carbon nanotubes in polymers. *Beilstein Journal of Nanotechnology* **2016**, *7*, 1174-1196. DOI: 10.3762/bjnano.7.109.

(9) Reibold, M.; Paufler, P.; Levin, A. A.; Kochmann, W.; Pätzke, N.; Meyer, D. C. Carbon nanotubes in an ancient Damascus sabre. *Nature* **2006**, *444* (7117), 286-286. DOI: 10.1038/444286a.

(10) Purohit, R.; Purohit, K.; Rana, S.; Rana, R. S.; Patel, V. Carbon Nanotubes and Their Growth Methods. *Procedia Materials Science* **2014**, *6*, 716-728. DOI: https://doi.org/10.1016/j.mspro.2014.07.088.

(11) Arora, N.; Sharma, N. N. Arc discharge synthesis of carbon nanotubes: Comprehensive review. *Diamond and Related Materials* **2014**, *50*, 135-150. DOI: https://doi.org/10.1016/j.diamond.2014.10.001.

(12) Filchakova, M.; Saik, V. *Single-walled carbon nanotubes: structure, properties, applications, and health & safety*. 2021. https://tuball.com/articles/single-walled-carbon-nanotubes

(13) Choudhary, V.; Singh, B. P.; Mathur, R. B. Carbon Nanotubes and Their Composites. InTech: 2013.

(14) Luanpitpong, S.; Wang, L.; Rojanasakul, Y. The effects of carbon nanotubes on lung and dermal cellular behaviors. *Nanomedicine (London, England)* **2014**, *9* (6), 895-912. DOI: 10.2217/nnm.14.42 PubMed.

(15) Allegri, M.; Perivoliotis, D. K.; Bianchi, M. G.; Chiu, M.; Pagliaro, A.; Koklioti, M. A.; Trompeta, A.-F. A.; Bergamaschi, E.; Bussolati, O.; Charitidis, C. A. Toxicity determinants of multi-walled carbon nanotubes: The relationship between functionalization and agglomeration. *Toxicology Reports* **2016**, *3*, 230-243. DOI: https://doi.org/10.1016/j.toxrep.2016.01.011.

(16) Eatemadi, A.; Daraee, H.; Karimkhanloo, H.; Kouhi, M.; Zarghami, N.; Akbarzadeh, A.; Abasi, M.; Hanifehpour, Y.; Joo, S. W. Carbon nanotubes: properties, synthesis, purification, and medical applications. *Nanoscale Research Letters* **2014**, *9* (1), 393. DOI: 10.1186/1556-276X-9-393.

(17) Attaf, B. *ON THE APPLICATION OF CARBON NANOTUBE-BASED COMPOSITE MATERIALS FOR SMART DESIGN OF WIND TURBINE BLADES*; 2016.

(18) Bocharov, G. S.; Eletskii, A. V. Theory of Carbon Nanotube (CNT)-Based Electron Field Emitters. *Nanomaterials (Basel, Switzerland)* **2013**, *3* (3), 393-442. DOI: 10.3390/nano3030393 PubMed.

(19) Liu, C.; Cheng, H.-M. Controlled Growth of Semiconducting and Metallic Single-Wall Carbon Nanotubes. *Journal of the American Chemical Society* **2016**, *138* (21), 6690-6698. DOI: 10.1021/jacs.6b00838.

(20) Mikulski, S.; Tomczewski, A. Use of Energy Storage to Reduce Transmission Losses in Meshed Power Distribution Networks. *Energies* **2021**, *14* (21). DOI: 10.3390/en14217304.

(21) CheapTubes. *Multi Walled Carbon Nanotubes*. Cheap Tubes, 2022. https://www.cheaptubes.com/product-category/multi-walled-carbon-nanotubes/

(22) Kharisov, B.; Kharissova, O. Variations of interlayer spacing in carbon nanotubes. RSC Adv.: 2014; Vol. 4.

(23) Shen, C.; Brozena, A. H.; Wang, Y. Double-walled carbon nanotubes: Challenges and opportunities. *Nanoscale* **2011**, *3* (2), 503-518, 10.1039/C0NR00620C. DOI: 10.1039/C0NR00620C.

(24) Nurazzi, N. M.; Sabaruddin, F. A.; Harussani, M. M.; Kamarudin, S. H.; Rayung, M.; Asyraf, M. R. M.; Aisyah, H. A.; Norrrahim, M. N. F.; Ilyas, R. A.; Abdullah, N.; et al. Mechanical Performance and Applications of CNTs Reinforced Polymer Composites—A Review. *Nanomaterials* **2021**, *11* (9). DOI: 10.3390/nano11092186.

(25) Jyoti, J.; Basu, S.; Singh, B. P.; Dhakate, S. R. Superior mechanical and electrical properties of multiwall carbon nanotube reinforced acrylonitrile butadiene styrene high performance composites. *Composites Part B: Engineering* **2015**, *83*, 58-65. DOI: https://doi.org/10.1016/j.compositesb.2015.08.055.

(26) Vázquez, E.; Prato, M. Carbon Nanotubes and Microwaves: Interactions, Responses, and Applications. *ACS Nano* **2009**, *3* (12), 3819-3824. DOI: 10.1021/nn901604j.

(27) Chen, X.; Liu, H.; Hu, D.; Liu, H.; Ma, W. Recent advances in carbon nanotubes-based microwave absorbing composites. *Ceramics International* **2021**, *47* (17), 23749-23761. DOI: https://doi.org/10.1016/j.ceramint.2021.05.219.

(28) Li, Y.; Chen, C.; Pan, X.; Ni, Y.; Zhang, S.; Huang, J.; Chen, D.; Zhang, Y. Multiband microwave absorption films based on defective multiwalled carbon nanotubes added carbonyl iron/acrylic resin. *Physica B: Condensed Matter* **2009**, *404* (8), 1343-1346. DOI: https://doi.org/10.1016/j.physb.2008.12.015.

(29) Coleman, J. N.; Khan, U.; Blau, W. J.; Gun'ko, Y. K. Small but strong: A review of the mechanical properties of carbon nanotube–polymer composites. *Carbon* **2006**, *44* (9), 1624-1652. DOI: https://doi.org/10.1016/j.carbon.2006.02.038.

(30) Sulong, A. B.; Muhamad, N.; Sahari, J.; Ramli, R.; Deros, B. M.; Park, J. Conductivity Behavior of Chemical Functionalized MWCNTs Epoxy Nanocomposites. European Journal of Scientific Research: 2009; Vol. 29, pp 13-21.

(31) Long, C. The Effect of Functionalized Multiwalled Carbon Nanotubes on The Mechanical And Rheological Properties of Polystyrene/Nanotube Composites. Electronic Theses and Dissertations: 2013; Vol. 898.

(32) Yang, C.; Lin, Y.; Nan, C. W. Modified carbon nanotube composites with high dielectric constant, low dielectric loss and large energy density. *Carbon* **2009**, *47* (4), 1096-1101. DOI: https://doi.org/10.1016/j.carbon.2008.12.037.

(33) González, M.; Mokry, G.; de Nicolás, M.; Baselega, J.; Pozuelo, J. Carbon Nanotube Composites as Electromagnetic Shielding Materials in GHz Range. IntechOpen: 2016.

(34) Hussein, M. I.; Jehangir, S. S.; Rajmohan, I. J.; Haik, Y.; Abdulrehman, T.; Clément, Q.; Vukadinovic, N. Microwave Absorbing properties of metal functionalized-CNT-polymer composite for stealth applications. *Scientific Reports* **2020**, *10* (1), 16013. DOI: 10.1038/s41598-020-72928-1.

(35) Liu, S.-H.; Hou, H.-Y.; Shu, C.-M. Thermal hazard evaluation of the autocatalytic reaction of benzoyl peroxide using DSC and TAM III. *Thermochimica Acta* **2015**, *605*, 68-76. DOI: https://doi.org/10.1016/j.tca.2015.02.008.

(36) Kertesz, M. Pancake Bonding: An Unusual Pi-Stacking Interaction. *Chemistry – A European Journal* **2019**, *25* (2), 400-416, https://doi.org/10.1002/chem.201802385. DOI: https://doi.org/10.1002/chem.201802385

(37) Shrivastava, A. 1 - Introduction to Plastics Engineering. In *Introduction to Plastics Engineering*, Shrivastava, A. Ed.; William Andrew Publishing, 2018; pp 1-16.

(38) Gracia-Fernández, C.; Álvarez-García, A.; Gómez-Barreiro, S.; López-Beceiro, J.; Artiaga, R. Temperature simulation of three-point bending geometry in a dynamic mechanical analyzer. *Polymer Testing* **2021**, *93*, 106895. DOI: https://doi.org/10.1016/j.polymertesting.2020.106895.

(39) Introduction to Dynamic Mechanical Testing for Rubbers and Elastomers. TAInstruments. http://www.tainstruments.com/wp-content/uploads/Introduction-to-Dynamic-Mechnical-Analysis_Akron-Workshop.pdf

APPENDIX

Raman Spectroscopy

The peaks at 1375 and 1500 cm^{-1}, the D and G-band, are the primarily vibrational modes of interest for the characterization of carbon nanotube. There is also a peak at 2700 cm^{-1} called the G^1-band that is correlated to vibrational stretching of carbon that are in-plane with the CNT structure. In Figure 25, the G^1-band can be seen along with broad stretching from 3000 to 2400 cm^{-1}. This type of stretching usually correlates to moisture caused from vibrational stretching between oxygen and hydrogen atoms. The samples were dried overnight at 90°C, but moisture absorption could have occurred during sample preparation for Raman spectroscopy.

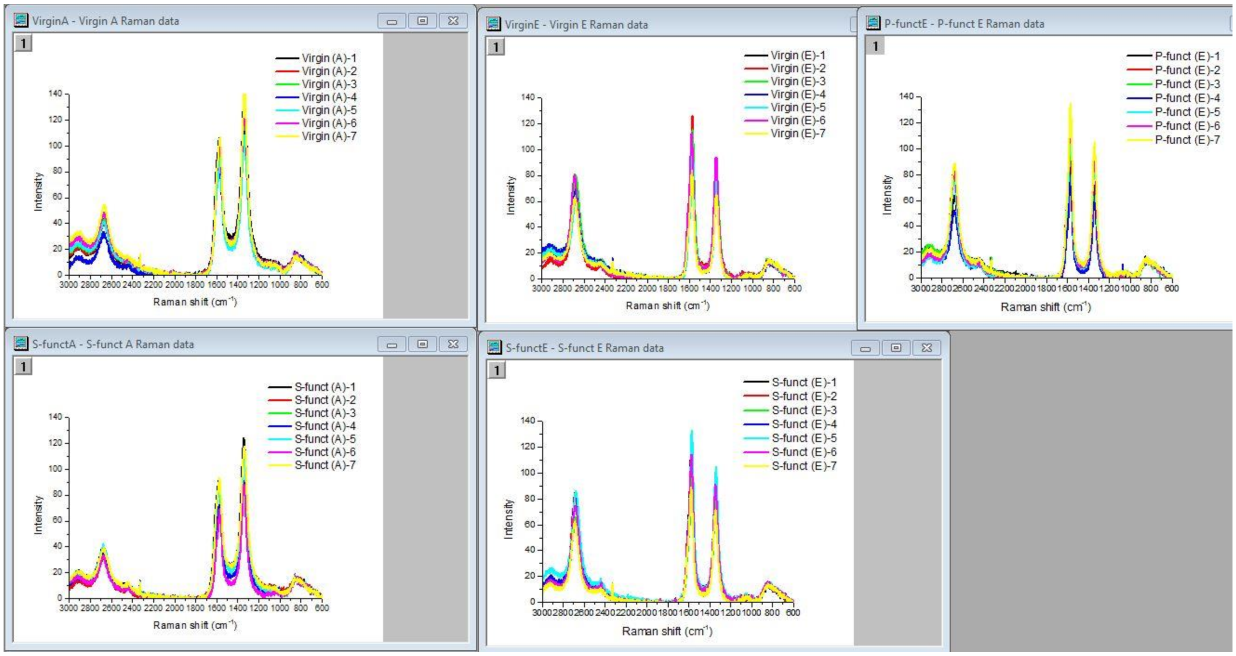

Figure 25. Raman spectroscopy data for all CNTs. The full spectrum is displayed to show D, G, and G^1-band stretching.

The presence of hydroxyl groups during a Grignard reaction would be an explanation as to why the CNTs were not functionalized to the extent of 2% of all carbons. Grignard reagent reaction mechanisms are based upon using partially charged magnesium and bromine salts as leaving groups to functionalize covalently bonded carbons. If hydroxyl groups are present in the CNT structure or any moisture is present, the Grignard reagent will favor the acidic hydrogen. This favored reaction towards hydroxyl groups is based on the partial charge that oxygen has and its ability to lose the hydrogen.

Tensile Strength Testing

Tensile strength testing was experimented with using a TestResources Tensile Strength Tester. The standard "dog bone" shape that is commonly used for tensile strength testing of composites was too large and would have taken too much product to produce multiple replicates. Tensile strength testing was carried out using the thin strips prepared in the thermal hydraulic press. The composites did not consistently break in the middle of the clamps, and many broke where the metal clamps were squeezing the composite. This leads to inconsistent data collection so was not included in the body of the thesis.

It should be noted that it was impossible to remove composites containing free radical initiators from the thin strip mold, so data collection for tensile strength of BPO containing composites was not even attempted. The composites containing functionalized Sample A CNTs were noticeably more brittle than composites containing Sample E CNTs. This observation does not have analytical data to correspond but is something that can be used to further characterize the CNT composites.